Biosensing and Biomedicine
https://www.sciltp.com/journals/bab

Review

Functional MOF-Mediated Platforms for Potentiating Tumor Hyperthermia: A Review

Diyi Feng and Liqin Ge *

State Key Lab of Digital Medical Engineering, School of Biological Science and Medical Engineering, Southeast University, Nanjing 211189, China
* Correspondence: lqge@seu.edu.cn

How To Cite: Feng, D.; Ge, L. Functional MOF-Mediated Platforms for Potentiating Tumor Hyperthermia: A Review. *Biosensing and Biomedicine* **2026**, *1*(1), 3.

Received: 18 May 2026
Revised: 27 May 2026
Accepted: 9 June 2026
Published: 18 June 2026

Abstract: Tumor hyperthermia represents a minimally invasive therapeutic modality designed to selectively eliminate cancer cells or augment the efficacy of combination regimens via localized temperature elevation. Conventional interventions, including surgical resection, radiotherapy (RT), and chemotherapy (CT) are constrained by intrinsic tumor heterogeneity, acquired drug resistance, and the complex tumor microenvironment, factors that collectively limit therapeutic outcomes. In this context, localized hyperthermia provides a physical mechanism to disrupt malignant cells while concurrently enhancing chemotherapeutic penetration and potentiating antitumor immune responses. Metal-organic frameworks (MOFs) have recently emerged as highly versatile platforms for tumor hyperthermia owing to their precisely tunable three-dimensional porous structures, diverse metal node compositions, and adaptable surface functionalization capabilities. These materials can directly convert light or MW energy into thermal energy and can also function as carriers for chemotherapeutic drugs or microwave (MW) sensitizers, thereby enabling multimodal synergistic interventions. This review presents a comprehensive analysis of recent progress in MOF-based photothermal therapy (PTT) and microwave hyperthermia (MWH), with particular emphasis on material design, mechanistic insights into heat generation, and strategies for functional integration. By systematically evaluating intrinsic, composite, and derived MOF systems, the review seeks to establish a theoretical and materials science framework for the rational development of efficient, controllable, and clinically translatable MOF-based tumor hyperthermia platforms.

Keywords: MOFs; tumor hyperthermia; photothermal therapy; microwave hyperthermia; functionalized materials; combination therapy

1. Introduction

Malignant tumors remain one of the leading causes of death worldwide [1]. The global incidence and mortality of cancer are projected to increase steadily, with annual new cases exceeding 29 million and cancer-related deaths approaching 10 million in recent epidemiological reports [2]. Surgery [3], radiotherapy (RT) [4], and chemotherapy (CT) [5] remain the mainstay of clinical cancer treatment. However, their therapeutic performance is often compromised by tumor heterogeneity [6], therapeutic resistance [7], and the complexity of the tumor microenvironment (TME) [8]. Tumor heterogeneity extends beyond interpatient genomic variation and includes intratumoral diversity in metabolic state, vascular structure, and immune infiltration [9]. These biological variations lead to markedly different treatment responses across patients and even among distinct regions within the same tumor. In addition to limited efficacy, conventional therapies are frequently associated with substantial adverse effects [10]. Chemotherapeutic drugs often damage normal proliferating tissues because of insufficient

tumor selectivity [11], whereas RT may cause collateral injury to surrounding organs and dose-limiting toxicity [12]. These challenges are particularly evident in advanced, recurrent, or treatment-resistant malignancies, where standard regimens fail to achieve durable tumor control [13]. These limitations have stimulated increasing interest in therapeutic strategies that provide localized tumor control, reduced systemic toxicity, and the potential for integration with conventional treatment modalities.

Tumor hyperthermia has attracted increasing attention as an adjuvant anticancer modality because it enables local thermal intervention through externally applied physical energy [14]. Depending on the temperature range and biological outcome, hyperthermia can generally be divided into thermal ablation and mild hyperthermia. Thermal ablation, typically performed at temperatures above 55 °C [15], induces rapid and irreversible damage to proteins, membranes, and cellular structures, making it more suitable for superficial or well-localized tumors, such as skin tumors and selected breast lesions [16]. Mild hyperthermia, typically conducted at 39–45 °C [17], produces sublethal thermal stress rather than immediate coagulative destruction. By disrupting proteostasis [18], impairing mitochondrial function [19], activating stress-response pathways [20], and modulating antitumor immunity [21], mild hyperthermia can sensitize tumors to CT [22] and immunotherapy (IT) [23]. Moreover, mild heating can enhance drug penetration into tumor tissues, increase tumor-cell susceptibility to chemotherapeutic drugs [24], and modulate heat shock protein-related immune responses, thereby improving the efficacy of combination therapy [25]. However, the therapeutic performance of hyperthermia is still constrained by several key barriers. For deep-seated tumors, precise and homogeneous heat deposition remains difficult to achieve. Inadequate heating at tumor margins, insufficient thermal accumulation in poorly perfused or heterogeneous regions, and unintended injury to adjacent normal tissues may all compromise therapeutic efficacy and safety [26]. In addition, repeated or prolonged thermal exposure can induce thermotolerance [27], which is closely associated with heat shock protein upregulation [28], enhanced antioxidant capacity [29], and microenvironmental buffering effects [30]. These adaptive mechanisms reduce the sensitivity of tumor cells to subsequent thermal stress. Hyperthermia is therefore increasingly positioned as a component of multimodal cancer therapy rather than as an independent treatment modality. Effective integration with CT [31], RT [32], or IT [33] requires material systems that can coordinate thermal energy conversion, tumor-selective accumulation, controlled therapeutic release, and modulation of relevant biological responses [34]. However, conventional photothermal and microwave-responsive nanomaterials often show uneven thermal distribution [35], limited tumor specificity [36], and suboptimal biocompatibility [37], particularly in deep-seated tumor settings. These limitations have motivated the development of advanced therapeutic materials capable of coupling efficient heat generation with targeted delivery and stimuli-responsive activation, thereby improving the spatial precision and translational feasibility of tumor hyperthermia.

Metal-organic frameworks (MOFs) have emerged as highly adaptable porous materials for the development of next-generation hyperthermia platforms. Constructed through the coordination-driven assembly of metal nodes and organic ligands, MOFs possess well-defined three-dimensional pore networks [38], tunable pore dimensions [39], large surface areas [40], and adjustable framework stability [41]. In addition, their surfaces can be chemically modified to improve colloidal stability, biological compatibility, and tumor-interactive functions [42]. These characteristics distinguish MOFs from conventional inorganic nanoparticles or polymeric carriers, which often offer more limited structural programmability.

In hyperthermia, MOFs can contribute to both energy conversion and therapeutic integration. The metal nodes or conjugated ligands may directly participate in optical or MW energy absorption, enabling intrinsic heat generation under external stimulation [43]. Their ordered pore systems also provide confined spaces for incorporating chemotherapeutic drugs [44], photosensitizers [45], MW sensitizers [46], or other functional molecules, thereby facilitating the construction of combination therapy platforms. Beyond pristine MOFs, derivative strategies such as carbonization, sulfidation, or oxidation can further enhance thermal stability [47] and energy-conversion efficiency [48]. Meanwhile, magnetic-metal doping [49] and surface engineering [50] can introduce imaging functionality, supporting tumor visualization and image-guided thermal intervention, especially for deep-seated tumors [51]. Tumor-selective delivery represents another important advantage of MOF-based systems. Surface engineering with polyethylene glycol [52], targeting peptides [53], or erythrocyte membrane coating [54] can prolong circulation, reduce premature clearance [55], and improve interactions with tumor vasculature or cancer cell surface receptors [56]. Such modifications increase intratumoral accumulation of hyperthermia drugs [57], improving spatial selectivity [58] while reducing nonspecific thermal injury to surrounding healthy tissues [59]. When coupled with stimulus-responsive drug release, this targeted delivery can further strengthen the therapeutic outcome of hyperthermia-based combination treatment [60]. Therefore, the integration of structural tunability, imaging compatibility, and tumor-targeting capability makes MOFs particularly attractive for constructing precise and multifunctional tumor hyperthermia platforms.

Accordingly, MOFs hold considerable promise for tumor hyperthermia owing to their structural programmability and functional adaptability (Figure 1). Through rational materials design, MOF-based systems can be developed as intrinsic, composite, or derived platforms to meet different requirements for thermal responsiveness, therapeutic integration, and multimodal combination treatment. This review summarizes recent advances in MOF-based platforms for PTT and MWH, with emphasis on hyperthermia mechanisms, functional integration strategies, and translational prospects. By linking materials design with therapeutic performance, this review aims to provide a materials-oriented perspective for the development of MOF-based hyperthermia platforms.

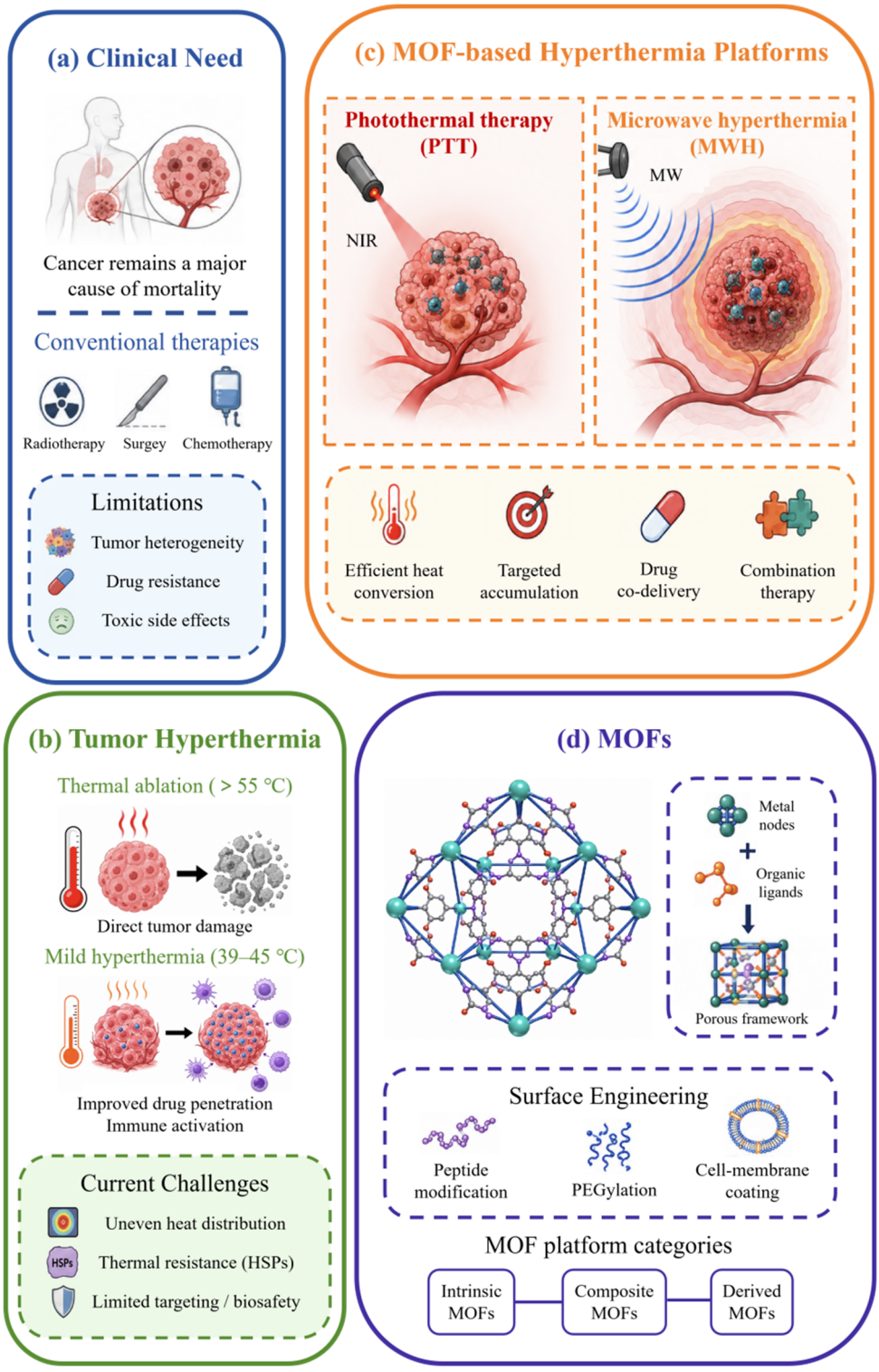

Figure 1. MOF-based platforms for tumor hyperthermia. (**a**) Major limitations of conventional cancer therapies; (**b**) Classification of tumor hyperthermia and key challenges associated with thermal treatment; (**c**) Functional roles of MOF-based platforms in hyperthermia-mediated cancer therapy; (**d**) Structural features and representative categories of MOF materials.

2. The Structure of MOF-Based Materials

The therapeutic performance of MOF-based materials is determined by the coordinated roles of metal nodes and organic ligands [61]. Metal nodes can impart redox activity [62], catalytic capability [63], magnetic responsiveness [64], MW sensitization [65], or imaging functions [66], whereas organic ligands may contribute through light absorption [67] and redox activity [68]. The intrinsic porosity of MOFs further enables the incorporation of diverse functional components, including chemotherapeutic drugs [69], photosensitizers [70], enzymes [71], and immunomodulatory molecules [72]. These structural attributes provide the basis for understanding how MOF-based hyperthermia platforms convert external energy into localized heat, initiate cellular injury, regulate the TME, and coordinate combination therapy. Accordingly, this section focuses on the compositional and architectural features of MOF-based materials.

The structural and functional diversity of MOF-based materials originates from the deliberate integration of metal nodes and organic linkers. Metal nodes serve as the inorganic connectivity centers of MOF frameworks and commonly include high-valence metals such as Zr, Ti, and Hf [73], transition metals such as Fe, Cu, and Mn [74], as well as rare-earth elements such as Gd and Eu that can impart imaging capability or specific energy-responsive behavior [75]. The choice of metal node not only governs coordination stability, crystal topology, degradation behavior, and *in vivo* metabolic fate, but also endows MOFs with redox activity, Fenton-like catalytic capacity, magnetic responsiveness, MW sensitization, and MRI/CT imaging functions [76]. According to the characteristics of their metal nodes, MOF-based materials can be broadly categorized into high-valence metal MOFs, transition-metal MOFs, magnetic MOFs, and multimetallic MOFs. High-valence metal MOFs, represented by Zr, Ti, and Hf-based frameworks, generally possess high charge density and readily form strong metal-oxygen coordination bonds with carboxylate or phosphonate-containing ligands. These features usually confer excellent hydrolytic and thermal stability, making such frameworks suitable for constructing well-defined theranostic platforms with controllable porosity and surface chemistry [77]. In contrast, transition-metal MOFs based on Fe, Cu, Mn, and related nodes exhibit accessible redox cycling and efficient electron-transfer capability. These features allow them to participate directly in Fenton or Fenton-like reactions, GSH depletion, and redox homeostasis disruption [78]. Magnetic MOF composites rely on Fe, Mn, or Co-containing nodes, or on incorporated magnetic nanophases such as Fe_3O_4 and ferrites, to dissipate externally applied energy through magnetic loss, dielectric loss, and interfacial polarization under alternating magnetic fields or MW irradiation. These systems can also be integrated with MRI to enable imaging-guided therapy and treatment monitoring [79]. Multimetallic MOFs further expand this design space by incorporating two or more metal centers within a single framework. The resulting electronic coupling and functional complementarity can simultaneously promote thermal conversion, ROS generation, GSH depletion, hypoxia modulation, drug release, and diagnostic imaging. Organic ligands constitute another critical determinant of MOF function. Carboxylate linkers, porphyrinic ligands, imidazolate linkers, ferrocene-containing ligands, and other π-conjugated molecules are commonly used to regulate framework geometry, pore dimensions, hydrophilicity, surface chemistry, and electronic structure [80]. In particular, extended π-conjugation, metal–ligand charge transfer, and nonradiative relaxation pathways can enhance the response of MOFs to near-infrared light, MW irradiation, or other external energy inputs [81]. Therefore, MOF-based materials should not be regarded merely as passive drug carriers. Instead, they represent highly programmable organic-inorganic hybrid platforms in which metal-node selection, linker engineering, pore-structure regulation, and surface functionalization can be coordinated to achieve precise control over therapeutic, diagnostic, and energy-conversion functions.

In MOF systems, structural features and material performance are intrinsically linked through the coordinated roles of metal nodes and organic linkers. Metal nodes act as secondary building units that define the framework topology, connectivity, and coordination environment, thereby shaping the overall structural robustness of the material [82]. Organic linkers provide the geometric and chemical scaffolds that determine pore size, channel architecture, pore-wall chemistry, and the spatial arrangement of active sites [83]. As a result, the properties of MOFs emerge from the integrated framework architecture rather than from the isolated characteristics of individual components. The chemical identity of the metal node is a major determinant of both structural stability and therapeutic functionality. Metal valence, coordination preference, Lewis acidity, redox activity, and magnetic behavior collectively influence framework integrity under physiological conditions and dictate whether the material can participate in catalytic therapy, redox modulation, magnetic resonance imaging, or MW sensitization [84]. This is particularly important for tumor hyperthermia, where the metal center may serve not only as a structural anchor but also as an active site for ROS generation, glutathione depletion, magnetic response, or energy dissipation. Organic linkers provide a second level of functional regulation by tailoring pore architecture, optical absorption, charge transfer, and surface chemistry [85]. Extended aromatic carboxylate linkers can enlarge pore apertures and increase accessible surface area, thereby improving the loading of chemotherapeutic agents, photosensitizers, or

microwave sensitizers [86]. Linkers bearing amino, imidazole, pyridine, or other functional groups can further modulate hydrophilicity, surface charge, and interactions with proteins, membranes, and tumor-associated biological interfaces [87]. Thus, organic linkers should not be regarded merely as structural bridges that maintain framework integrity; they are functional components that critically determine the optical responsiveness, interfacial behavior, and biological performance of MOFs.

The defining feature of MOFs, distinguishing them from conventional nanomaterials, lies in the highly ordered porous lattices constructed through the cooperative design of metal nodes and organic ligands [88]. These crystalline frameworks exhibit long-range periodicity [89] and structural regularity [90], providing stable channels for the encapsulation and controlled release of therapeutic drugs [91], photosensitizers [92], or microwave-responsive molecules [93]. Additionally, the interface between metal nodes and ligands generates polarization effects that facilitate the efficient conversion of external energy into heat [94], enabling localized hyperthermic effects in tumor tissues [95]. MOF lattices are assembled by linking metal ions or clusters via organic ligands into three-dimensional networks [96], yielding frameworks with high mechanical stability [97], high surface areas [98], and hierarchical porosity [99]. The extensive accessible surface area amplifies interactions with optical or electromagnetic fields, enhancing energy absorption efficiency [100]. Pore architecture represents another critical structural determinant linking MOF composition to hyperthermia performance. Pore sizes can be tuned continuously from micropores (<2 nm) [101] to mesopores (2–50 nm) [102] and beyond, controlling not only the loading efficiency of photothermal or MW sensitizers [103], but also the propagation and attenuation of electromagnetic waves within the material [104]. High surface area and accessible pore channels facilitate the incorporation of chemotherapeutic agents, photosensitizers, ionic liquids, gas donors, and immunomodulatory molecules, while enabling their release in response to pH, GSH, enzymes, light irradiation, or microwave stimulation. In MWH, the pore structure plays an additional role as a confined microenvironment for ions and polar molecules. The large internal surface areas and hierarchical channels increase multiple scattering and reflection of microwave energy within the material, while promoting high-frequency vibration, molecular collision, dipolar rotation, and polarization relaxation under the MW field [105]. These processes prolong the interaction between electromagnetic waves and the framework, thereby improving microwave-to-heat conversion efficiency [106]. Such hierarchical and porous structures are essential for hyperthermia applications, facilitating localized heat accumulation and sustained energy release within the TME [107]. Accordingly, MOF pores should not be regarded merely as passive reservoirs for drug storage. Instead, they constitute active structural domains that simultaneously support guest loading, stimulus-responsive release, energy deposition, and localized thermal-field formation. By regulating pore size, pore geometry, and channel connectivity, the adsorption behavior, molecular recognition, and functional responsiveness of MOFs can be further optimized.

Another critical structural attribute of MOFs is the diversity of interfacial electromagnetic behaviors. Unlike conventional photothermal or dielectric nanomaterials that rely primarily on a single loss mechanism, MOFs possess abundant metal–ligand interfaces [108], crystallographic boundaries [109], and defect sites [110]. These interfacial regions can support multiple energy dissipation pathways under alternating electromagnetic fields, including interfacial polarization [111], dipolar relaxation [112], free-carrier conduction [113], and localized current pathways [114]. The presence of transition-metal centers, polar linkers, and structural defects can markedly reshape the electromagnetic and catalytic properties of MOF-based materials. Transition-metal d orbitals can participate in electronic transitions [115] and enhanced polarizability [116], thereby strengthening the dielectric response of the framework. In addition, spatially heterogeneous charge distribution and localized charge accumulation promote dielectric dissipation, which facilitates the conversion of incident MW energy into heat. Defect structures, including missing linkers, metal vacancies, lattice mismatch, and heterometal incorporation, introduce additional electronic states and polarization centers that favor charge separation and energy dissipation [117]. These defect-mediated effects are highly relevant to hyperthermia, as they can enhance optical absorption and nonradiative relaxation in PTT, while increasing polarization loss, conductive loss, and interfacial loss in MWH [118]. In chemodynamic therapy (CDT), defect-rich frameworks may also expose more catalytically accessible metal sites, thereby improving H_2O_2 activation and ROS production [119]. Controlled defect engineering therefore provides an effective route to modulate thermal conversion, catalytic reactivity, and TME responsiveness. Nevertheless, the density and type of defects must be carefully regulated, as excessive structural disorder may weaken framework stability, accelerate metal-ion leakage, and increase potential biosafety risks. Beyond the crystalline framework, particle size, morphology, and surface chemistry further determine the biological behavior and therapeutic performance of MOF-based systems. Two-dimensional nanosheets, hollow structures, and core-shell architectures can improve heat generation and drug-release behavior by increasing accessible surface area, shortening diffusion pathways, and enhancing guest-loading efficiency [120]. Surface engineering through peptide conjugation, cell-membrane coating, or targeting-ligand modification can improve colloidal stability during circulation, reduce

nonspecific protein adsorption, and enhance recognition of tumor cells or TME [121]. These considerations indicate that the functional behavior of MOFs is dictated by both their internal coordination architecture and external biointerfacial properties, which jointly shape energy-conversion efficiency, delivery performance, and therapeutic efficacy [122,123] (Figure 2).

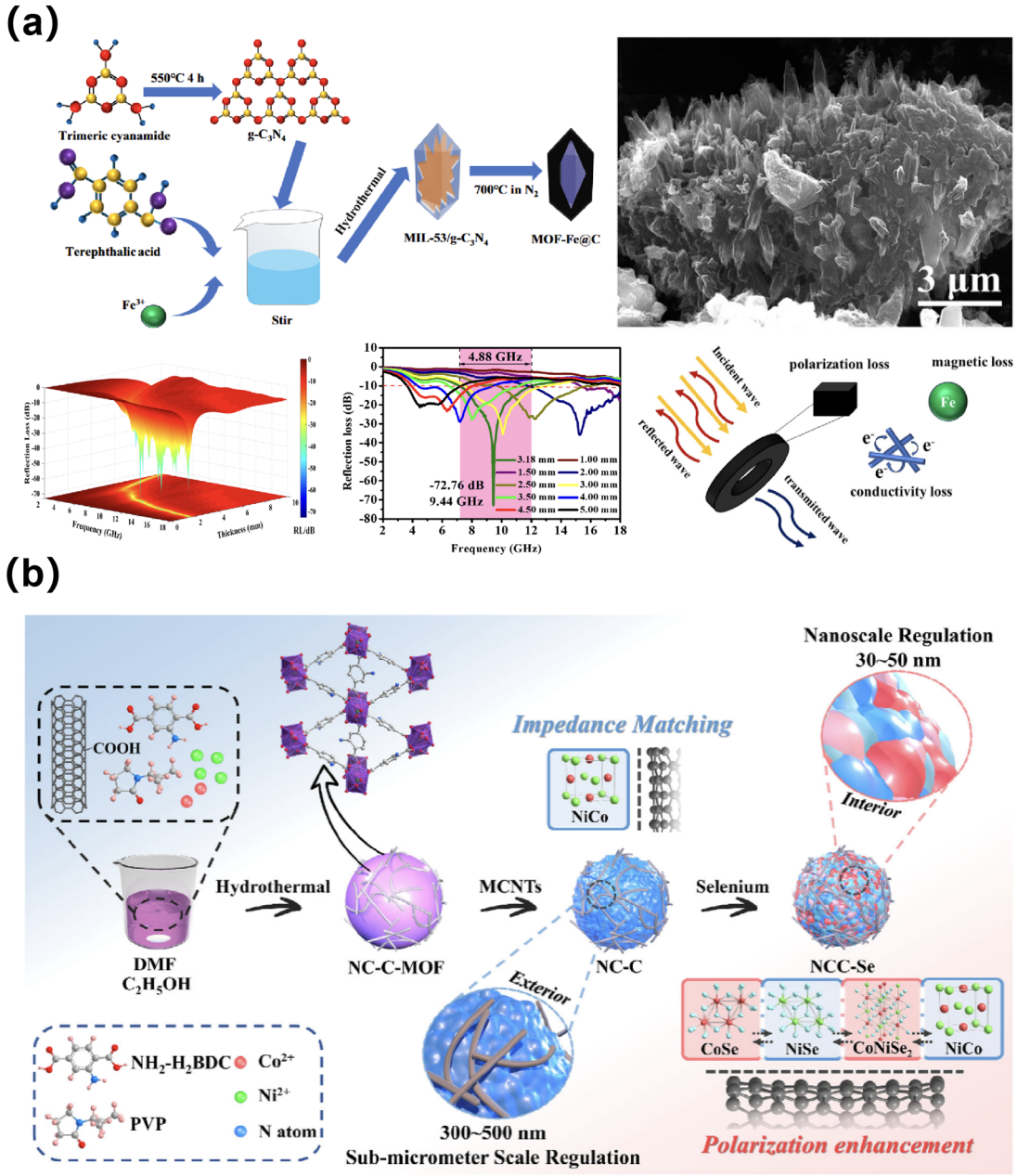

Figure 2. (**a**) MOF-Fe@C enhances microwave absorption through the combined effects of dielectric loss and magnetic loss from embedded magnetic nanoparticles [122], Copyright 2024, WILEY; (**b**) NCC-Se achieves optimized impedance matching via macroscale structural tuning, while microscale modifications within the material amplify attenuation properties [123], Copyright 2026, WILEY.

The structural tunability of MOFs represents a key advantage for their application in tumor hyperthermia. By selection of metal nodes and organic ligands, the crystallographic framework [124], pore morphology [125], and surface functionality [126] can be precisely modulated, allowing the design of platforms optimized for specific hyperthermia modalities. Incorporation of polar ligands enhances dipolar responses under microwave irradiation [127], transition-metal doping increases ROS generation [128], and magnetic elements introduce additional magnetic loss pathways [129], enabling combined dielectric and magnetic energy conversion. Luo et al. reported Fe-doped Cu-based bimetallic MOF nanoparticles (FCM) synthesized via a hydrothermal method, serving as nanoscale sensitizers for MW ablation and microwave-activated CDT in hepatocellular carcinoma. Fe incorporation into the Cu-MOF framework increased the density of active metal sites and metal–ligand interfaces, enhancing polarization

relaxation, dielectric loss, and MW energy dissipation. The Fe-associated magnetic centers further contributed to magnetic losses, collectively improving MW absorption and thermal conversion efficiency. Under MW irradiation, the porous FCM framework restricted the motion of ions and polar molecules, promoting localized heat generation, while the Fe/Cu bimetallic sites facilitated GSH depletion and Fenton reactions, boosting hydroxyl radical production and enabling synergistic MWH and CDT (Figure 3a) [130]. Compared with conventional inorganic thermal conversion materials, MOFs possess a chemically complex framework that often contains controllable defect sites, including ligand vacancies [131], metal vacancies [132], and lattice mismatches [133]. These defects serve as hotspots for electromagnetic energy dissipation, increasing local energy density and enhancing heat generation [134,135]. As a result, MOFs with abundant defect sites exhibit superior energy conversion efficiency and more pronounced localized temperature elevation, underscoring their potential as highly effective platforms for tumor hyperthermia.

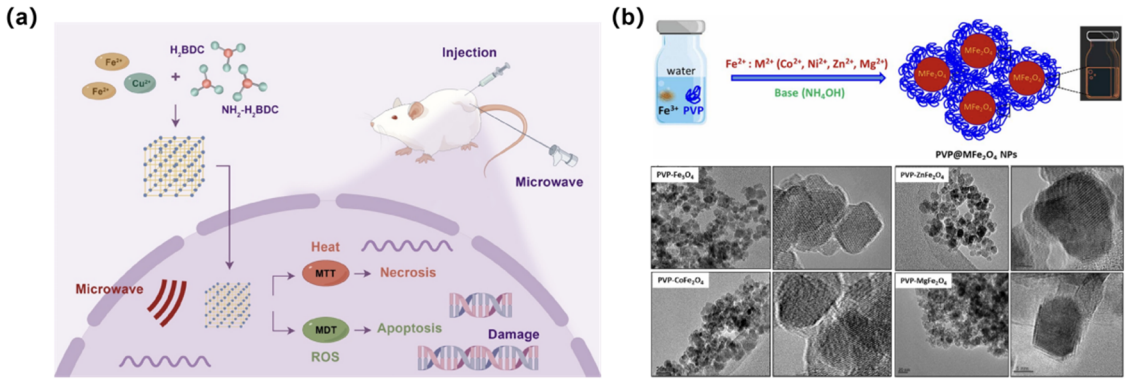

Figure 3. (**a**) Fe incorporation into a Cu-based MOF enhances both dielectric and magnetic losses, thereby improving microwave-to-heat conversion efficiency [130], Copyright 2024, RSC Publishing; (**b**) The incorporation of different divalent metal ions into an Fe-based MOF gives rise to distinct magnetothermal conversion behaviors [135], Copyright 2024, RSC Publishing.

The intrinsic structural features of MOFs establish a robust foundation for their use in tumor hyperthermia. These structures enable efficient thermal conversion, precise modulation of heat distribution, and enhanced energy deposition, while providing defined spatial and chemical sites for synergistic drug delivery and ROS amplification. Such properties have been consistently demonstrated in preclinical studies, positioning MOFs as versatile and high-potential materials for advanced thermal cancer therapies.

3. Classification of MOF-Based Materials

The primary advantage of MOF-based compounds in tumor hyperthermia lies in their highly tunable organic–inorganic hybrid structures. Based on the underlying mechanisms of thermal conversion and functional integration, MOFs for hyperthermia can be categorized into intrinsic MOFs, composite MOFs, and MOF-derived systems.

3.1. Intrinsic MOFs

Intrinsic MOFs are defined by their capacity to convert external energy into localized heat solely through their inherent chemical and crystallographic properties, without the need for exogenous photothermal or microwave sensitizers [136]. The fundamental mechanism relies on energy coupling and electron transfer between metal nodes and organic ligands [137]. High-valence metal centers provide not only structural stability under thermal or optical stimulation but also a well-defined coordination environment that facilitates efficient energy transfer across the framework [138]. In addition, the intrinsic porosity and large surface area of these MOFs promote uniform heat distribution within the material, enhancing the controllability of thermal effects while minimizing collateral damage to surrounding healthy tissues. Deng et al. synthesized ultrathin two-dimensional Zr-Fc MOF nanosheets for intrinsic PTT combined with CDT. The framework, composed of Zr–O clusters and ferrocene-dicarboxylate ligands, was not loaded with additional photothermal agents, the photothermal conversion was mediated by the electronic structure and coordination environment of MOFs. Zr-Fc MOF exhibited broadband absorption from 350–1350 nm and demonstrated efficient photothermal heating under 808 nm irradiation. The unique electronic properties of the ferrocene ligands, the metal–ligand coordination states, and the two-dimensional nanosheet morphology collectively enhanced nonradiative energy dissipation, endowing the material with robust intrinsic photothermal performance (Figure 4a) [139]. Beyond photothermal effects, intrinsic MOFs

can also respond to MW or alternating magnetic fields, where electronic polarization and valence-state cycling between metal nodes and ligands facilitate energy absorption and conversion [140]. Feng et al. reported a one-pot hydrothermal synthesis of Cu-doped Zr-MOF as a MW sensitizer for liver cancer therapy combining MWH and microwave dynamic therapy (MWDT). Without additional MW absorbers, the microporous structure and flexible framework of MOFs confined ions, promoting high-frequency vibrations and inelastic collisions under MW irradiation. This spatial confinement enabled efficient microwave energy dissipation and localized thermal conversion. Experiments demonstrated that Cu–Zr MOF achieved superior heating compared with Zr-MOF, indicating the synergistic enhancement of microwave-to-heat conversion through Cu doping and MOF confinement (Figure 4b) [141].

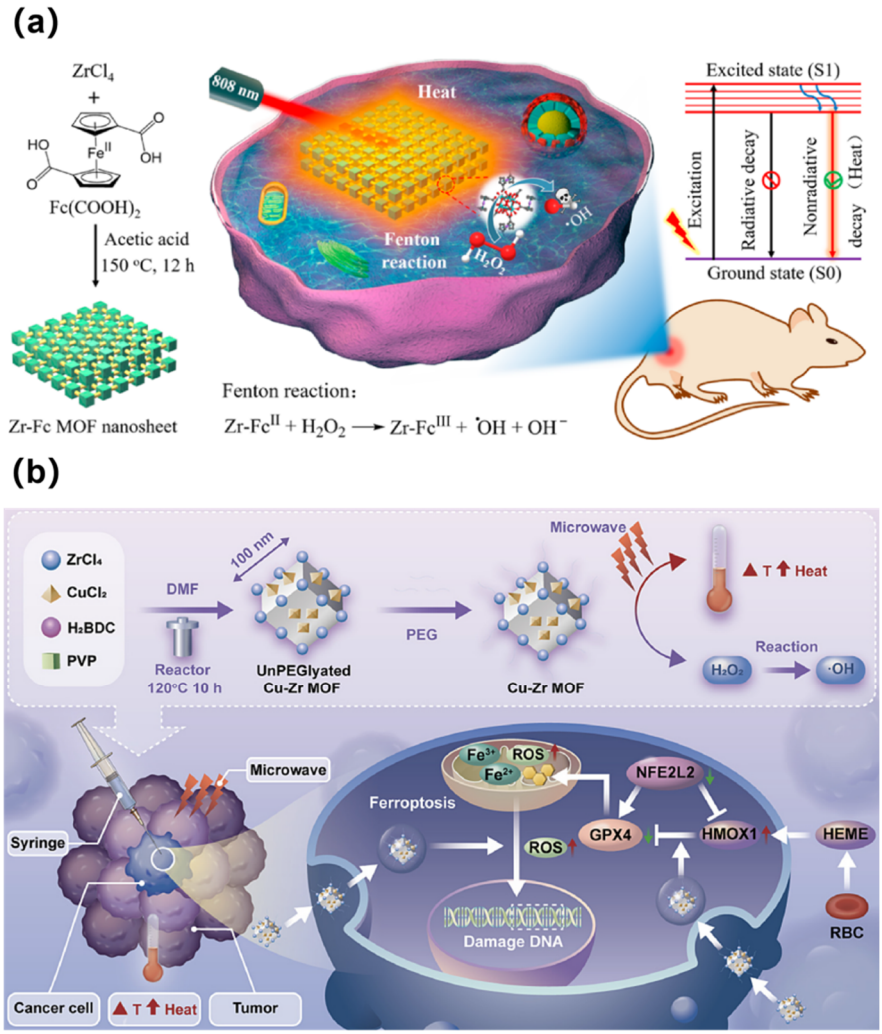

Figure 4. (**a**) Zr-Fc MOF nanosheets leveraging intrinsic photothermal properties to mediate PTT [139], Copyright 2020, ACS Publications; (**b**) Cu-Zr MOF utilizing microwave-responsive behavior to enhance MWH [141], Copyright 2023, Elsevier.

3.2. Composite MOFs

Composite MOFs enhance hyperthermia performance by incorporating exogenous functional agents within the pores or on the surfaces, achieving synergistic integration of energy conversion and therapeutic functionality [142]. Loading photothermal or microwave-sensitizing components within MOF channels not only increases absorption efficiency under optical or electromagnetic stimulation but also mitigates aggregation-induced performance loss and improves circulation stability and tumor-site retention [143]. Dinesh Kumar et al. developed a copper-doped ZIF-8 (Cu-ZIF-8) co-loaded with the photosensitizer ICG and the chemotherapeutic agent DOX, forming the IDCZ platform for combinational cancer therapy. Incorporation of ICG into the MOF channels not only enhanced near-infrared light absorption but also prevented aggregation-induced photobleaching, resulting in robust and sustained photothermal conversion. Upon NIR irradiation, the IDCZ microneedle patch achieved a rapid temperature increase up to 56 °C within 5 min, demonstrating excellent photothermal stability across multiple irradiation cycles [144].

Wang et al. developed a polydopamine-coated Fe-MOF-NH_2@Pt@PDA nanoplatform (FPP) for multimodal synergistic cancer therapy. The Fe-MOF-NH_2 framework was loaded with Pt nanoparticles, and PDA served as the primary photothermal agent. The coating of PDA significantly enhanced near-infrared (808 nm) absorption and ensured robust photothermal stability under repeated irradiation cycles. Upon NIR irradiation, FPP suspensions exhibited rapid temperature rises, with photothermal conversion efficiency reaching approximately 35.9%, confirming strong photothermal performance [145]. Moreover, composite MOFs can co-deliver chemotherapeutic drugs, allowing thermal stimuli to trigger localized drug release alongside direct tumor ablation, thereby enabling a coordinated PTT–CT response. Jiang et al. employed ZIF-8 as a MOF scaffold to encapsulate CuS nanoparticles as photothermal agents and co-loaded quercetin (QT), followed by FA–BSA surface modification to construct the FA–BSA/CuS@ZIF-8-QT platform for combined PTT and CT. The introduction of CuS endowed the ZIF-8 framework with pronounced near-infrared absorption, as pristine ZIF-8 exhibited negligible absorption across 700–1100 nm, confirming that CuS was the primary contributor to the photothermal conversion. The MOF scaffold enabled efficient QT loading and pH-responsive release, while FA–BSA modification enhanced colloidal stability, tumor targeting, and cellular uptake, integrating photothermal conversion, drug delivery, pH-triggered release, and active targeting into a single composite platform, thus enhancing synergistic PTT–CT efficacy (Figure 5a) [146]. Similarly, Ma et al. utilized Fe-MIL88B-NH_2 to host indocyanine green (ICG) via π–π stacking interactions, forming MOF@ICG nanocomposites for low-temperature PTT in combination with CDT and photodynamic therapy (PDT). MOF@ICG exhibited significantly enhanced near-infrared absorption over 700–900 nm and demonstrated effective, concentration and power-dependent temperature elevation under 808 nm irradiation, maintaining stability over multiple on/off laser cycles. Encapsulation of ICG within the MOF scaffold not only compensated for the limited intrinsic photothermal response of the original MOF but also allowed integration of NIR-induced photothermal conversion, ROS generation, and catalytic therapy within a single composite system (Figure 5b) [147]. Overall, composite MOFs provide a versatile platform that consolidates thermal energy conversion, controlled drug release, and ROS amplification, thereby improving both the efficacy and controllability of tumor hyperthermia.

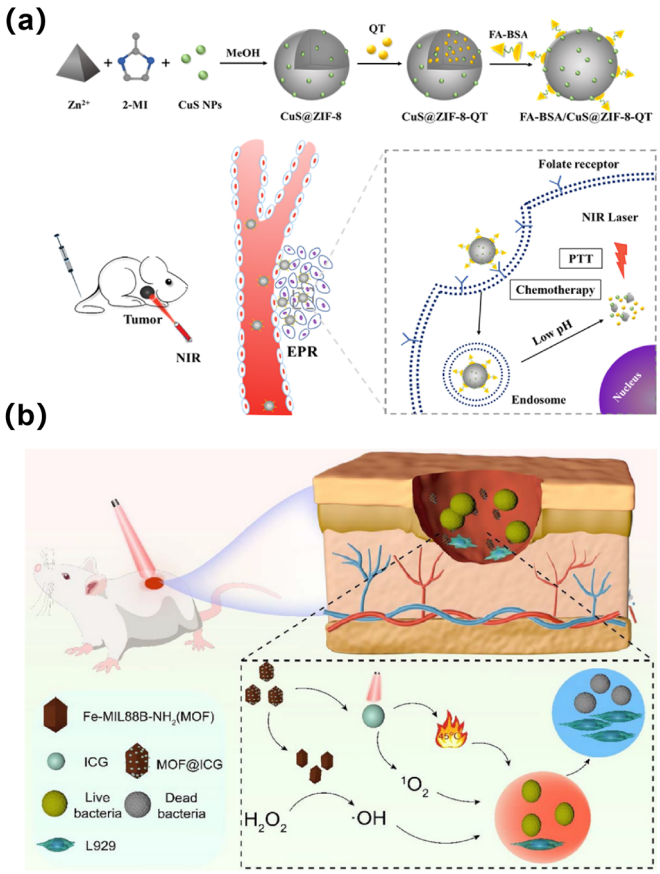

Figure 5. (**a**) FA–BSA/CuS@ZIF-8-QT nanoplatform, in which the incorporation of CuS nanodots endows the MOF with enhanced photothermal conversion [146], Copyright 2018, ACS Publications; (**b**) Fe-MIL88B-NH_2 loaded with ICG, providing the MOF with effective near-infrared photothermal responsiveness [147], Copyright 2024, RSC Publishing.

3.3. MOF-Derived Materials

Although MOF-derived materials and composite MOFs may both comprise multiple functional constituents, they are distinguished by fundamentally different formation mechanisms and structural identities. Composite MOFs are typically built around a structurally intact MOF host, with functional agents, such as photothermal compounds, photosensitizers, therapeutic drugs, ionic liquids, or inorganic nanocomponents, introduced into the pores, immobilized on the surface, or incorporated within an outer shell. In these systems, the parent MOF framework is largely retained and mainly functions as a porous host, spatial confinement scaffold, protective matrix, and stimulus-responsive delivery platform. MOF-derived materials, in contrast, originate from the chemical or thermal transformation of a parent MOF precursor. Processes such as carbonization, oxidation, sulfidation, pyrolysis, and etching reconstruct the original framework at the compositional and structural levels, yielding porous carbon, metal oxides, metal sulfides, or metal/carbon hybrid architectures [148]. Jiang et al. reported a MOF-derived, oxygen-deficient titanium dioxide nanoparticle platform (MCTx NPs) designed for combined photothermal and photodynamic-enhanced immunotherapy. The nanoparticles were synthesized via solid-state pyrolysis of MIL-125, followed by deposition of MnO_2 on the surface, creating a carbon matrix–TiO_2–MnO_2 composite with abundant oxygen vacancies (OVs). The MOF-derived structure endowed MCTx NPs with a highly porous architecture, facilitating uniform MnO_2 distribution and efficient NIR absorption. The introduction of OVs and the carbon matrix extended light absorption into the NIR-I/II region and improved electron–hole separation, resulting in enhanced ROS generation and a photothermal conversion efficiency of 37.9% under 808 nm irradiation [149]. Yue et al. designed a carbonized MOF/MoS_2 heterostructure (CMOF@MoS_2) with abundant lattice defects to enhance PTT performance. The CMOF was obtained by high-temperature carbonization of ZIF-8 nanoparticles, followed by *in situ* growth of MoS_2 nanosheets, forming a core–shell heterostructure with strong interfacial interactions. The abundant defects in both CMOF and MoS_2 layers reduced the electron diffusion barrier and facilitated rapid charge transfer across the interface. This built-in electric field at the CMOF@MoS_2 heterojunction promoted efficient separation of photo-excited electron–hole pairs under NIR irradiation, resulting in enhanced light-to-heat conversion efficiency. When integrated into a conductive hydrogel for self-powered sensing and on-demand PTT, CMOF@MoS_2 exhibited a photothermal conversion efficiency of 49.5%, surpassing that of either CMOF or MoS_2 alone, and demonstrated stable and repeatable heating over multiple cycles [150]. These derivatization processes can establish conductive or polarizable pathways within the material, promoting efficient conversion of external energy into heat and simultaneously improving ROS generation and the release of therapeutic drugs [151]. The classification of a material as MOF-derived should not be based simply on whether residual MOF components are present or whether the final product exhibits a composite-like architecture. The defining criterion is whether the functional phase is generated through *in situ* transformation of a MOF precursor, and whether the metal nodes, organic linkers, or pore framework of the parent MOF participate in the formation of the new functional structure.

On this basis, MOF-derived materials can be further divided into fully derived and partially derived systems. Fully derived materials refer to products in which the parent MOF framework largely loses its original crystallographic identity during thermal treatment or chemical conversion and is transformed into new phases, such as porous carbon, metal oxides, or metal/carbon composites [152]. For instance, Li et al. transformed ZIF-8 into hierarchical porous carbon nanoparticles (CNPs) via high-temperature carbonization at 900 °C, followed by hydrochloric acid etching to remove residual Zn and its oxides. This procedure not only disrupted the original MOF crystallinity to form graphitized and defect-rich carbon structures but also generated mesopores that increased specific surface area and improved pore structure. The resulting CNPs exhibited pronounced near-infrared absorption and high photothermal conversion efficiency; when loaded with L-arginine as a nitric oxide donor and coated with red blood cell membranes, the CNP-NO@RBCs system enabled photoacoustic imaging-guided synergistic PTT (Figure 6a) [153]. Partially derived materials, by contrast, are systems in which only selected metal nodes or surface regions of the parent MOF undergo *in situ* sulfidation, oxidation, or other chemical transformations to generate new functional phases, while certain features of the original MOF, such as morphology, pore architecture, or residual framework structure, are partially retained [154]. Geng et al. employed a partially *in situ* sulfidation strategy to convert porous Cu-MOF into CuS@Cu-MOF nanocomposites, which were subsequently PEGylated to yield CuS@Cu-MOF/PEG for photothermal and multimodal combination therapy. In this approach, CuS nanodots were formed within the MOF surface and pores while retaining the spindled morphology and porosity of the parent Cu-MOF. The incorporation of CuS markedly enhanced near-infrared absorption across 600–1100 nm, reflecting the contribution of CuS plasmonic effects. The composite preserved the drug-loading capability of the MOF, enabling doxorubicin encapsulation with accelerated release under acidic conditions, and facilitated Fenton-like ·OH generation through Cu catalysis, integrating PTT, CDT, CT, and

imaging guidance within a single MOF-derived platform (Figure 6b) [155]. These partially derived architectures represent a transitional category between composite MOFs and fully transformed MOF-derived materials. They preserve selected attributes of the parent framework, including guest-loading capacity and spatial confinement, while newly formed functional phases, such as metal sulfides, oxides, or related inorganic domains, provide enhanced photothermal conversion, MW responsiveness, or catalytic activity. In summary, MOF-derived materials offer a combination of structural robustness, improved thermal stability, and functional versatility. When further integrated with surface engineering strategies, they can enable targeted delivery and treatment-triggered drug release, making them attractive candidates for multimodal PTT and MWH against deep-seated tumors.

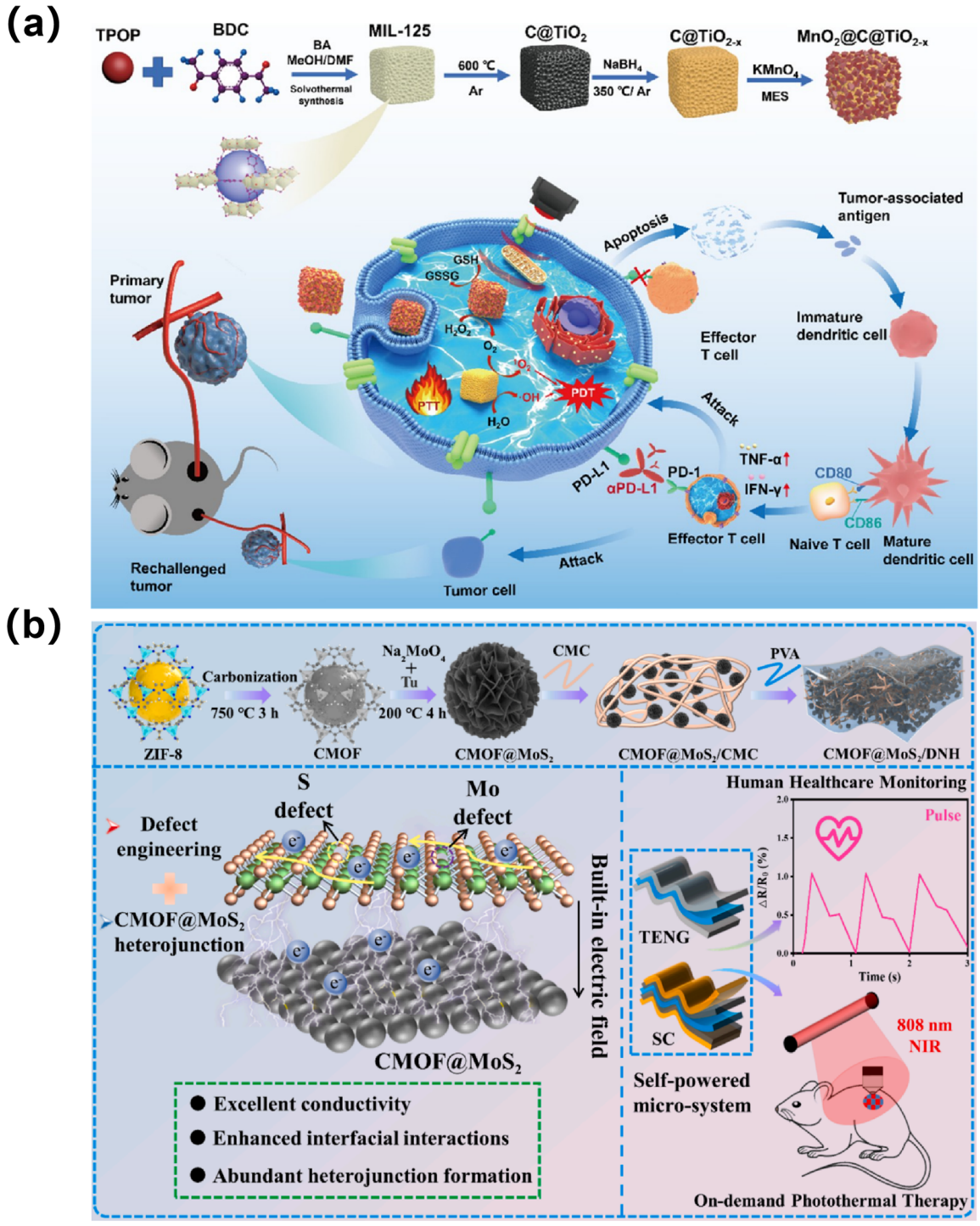

Figure 6. MOF-derived photothermal platforms for cancer therapy. (**a**) CMOF@MoS_2 heterojunction with defect engineering and enhanced interfacial interactions for improved photothermal performance [149], Copyright 2024, ACS Publications; (**b**) MnO_2@C@TiO_{2-x}-based system integrating PTT, PDT, ROS generation, and immune activation for synergistic tumor treatment [150], Copyright 2024, Elsevier.

The comparative analysis of intrinsic MOFs, composite MOFs, and MOF-derived materials reveals that their distinct structural architectures have direct implications for thermal conversion efficiency, biodegradation behavior, and therapeutic performance. Intrinsic MOFs generate photothermal or microwave-responsive effects primarily through the intrinsic electronic features of the framework, including metal–ligand charge transfer, linker conjugation, and interfacial polarization. Because their thermal response is derived from the framework itself rather than from incorporated exogenous sensitizers, intrinsic MOFs often provide a structurally well-defined platform with clear mechanistic origins. However, their energy-conversion efficiency may be limited by the inherent absorption capacity, charge-transfer efficiency, and energy dissipation pathways of the parent framework. Consequently, additional strategies, such as metal doping, linker engineering, defect modulation, or coupling with CDT, are frequently required to improve therapeutic efficacy [156]. Their biodegradation profiles are largely governed by coordination strength and TME responsiveness. High-valence metal frameworks, including Zr and Hf-based MOFs, generally exhibit greater structural stability but slower *in vivo* degradation, whereas transition-metal MOFs may dissociate more readily under acidic conditions, facilitating drug or metal-ion release while also raising concerns regarding premature framework decomposition and metal-related toxicity.

Composite MOFs, by contrast, achieve enhanced hyperthermia performance through the integration of exogenous functional components within an intact MOF host. Near-infrared absorbers such as CuS, ICG, and other photothermal agents can markedly improve optical absorption and photothermal conversion efficiency [157], whereas MW sensitizers such as ionic liquids can strengthen dielectric loss, ionic conduction, and microwave-to-heat conversion [158]. In these systems, the porous framework and shell structure of MOFs provide spatial confinement, improve the dispersion and stability of the functional components, and facilitate their *in vivo* delivery. From a therapeutic perspective, the principal advantage of composite MOFs lies in their capacity for multimodal integration, enabling hyperthermia to be combined with CT, CDT, IT, or imaging-guided treatment within a single platform. Such integration can enhance tumor ablation and compensate for the limitations of monotherapy. Nevertheless, the increased compositional complexity of composite MOFs introduces additional challenges, including batch-to-batch reproducibility, precise control of drug loading, predictable release kinetics, and long-term safety assessment. Their biodegradation behavior is also more heterogeneous, as framework disassembly, drug release, residual inorganic component clearance, and surface-coating metabolism may occur through different pathways and at different rates *in vivo* [159].

MOF-derived materials generally display stronger thermal stability, electrical conductivity, and energy-dissipation capacity as a consequence of structural transformation. Carbonization, oxidation, sulfidation, pyrolysis, or related derivatization processes can generate porous carbon frameworks, metal oxides, metal sulfides, or metal/carbon hybrid structures with enhanced photothermal conversion, microwave absorption, or magnetothermal responsiveness. Porous carbon domains, defect-rich structures, and metal/carbon interfaces can promote near-infrared absorption, nonradiative relaxation, conductive loss, and interfacial polarization, while metal oxides and sulfides may further contribute catalytic activity, magnetic responsiveness, or plasmonic absorption. These features make MOF-derived materials particularly attractive for high-efficiency thermal conversion platforms, especially when strong photothermal stability or MW absorption is required. Their therapeutic efficacy can also be amplified by residual metal active sites, porous matrices, and defect-mediated catalytic centers, which support ROS generation, drug loading, and imaging guidance [160]. However, the enhanced structural robustness may also complicate biodegradation and clearance. Compared with parent MOFs that can undergo gradual dissociation in acidic tumor or lysosomal environments, carbonized frameworks, metal sulfides, and metal/carbon composites are often less readily degradable and may pose risks of long-term tissue retention, chronic inflammatory responses, or sustained metal-ion release [161]. Therefore, although MOF-derived materials offer notable advantages in thermal conversion performance, their translational potential depends on rigorous evaluation of long-term biosafety, degradation pathways, and *in vivo* metabolism.

In summary, the classification of MOF-based materials for tumor hyperthermia is fundamentally guided by their mode of thermal activation and functional integration rather than by the specific type of metal node. Intrinsic MOFs exploit their native crystal and electronic structure to directly convert external energy into localized heat. Composite MOFs leverage the incorporation of exogenous agents to synergistically amplify thermal effects alongside drug release or ROS generation. MOF-derived materials achieve enhanced thermal stability and responsiveness through structural transformations such as carbonization, sulfidation, or oxidation. Framing the classification around functional mechanisms clarifies the performance differences among MOF platforms and provides actionable principles for designing and optimizing hyperthermia nanomaterials.

4. Applications of MOF-Based Materials in Tumor Hyperthermia

Depending on the type of external energy and the underlying heat-generation mechanism, MOF-based materials have been explored primarily in PTT and MWH. This section focuses on how structural design and functional integration in MOFs enhance energy conversion efficiency, improve tumor-specific accumulation, and elevate the overall therapeutic outcome.

4.1. PTT

PTT is a minimally invasive approach that converts absorbed light into heat to induce localized hyperthermia. In recent years, MOF-based materials have attracted considerable attention for PTT applications [162]. The therapeutic principle relies on near-infrared light (NIR) absorption, followed by non-radiative relaxation, to generate controlled heating at the tumor site. The resulting thermal stress can disrupt protein folding, compromise membrane integrity, impair mitochondrial function, and damage DNA, ultimately triggering apoptosis or necrosis in cancer cells [163]. MOFs offer significant advantages in this context due to their highly tunable lattice structures, porous structures, and programmable metal nodes and organic linkers, which collectively enhance photothermal conversion efficiency, thermal stability, and tumor targeting. Moreover, the porous structure facilitates uniform heat distribution within both the material and surrounding tumor tissue, improving the precision and safety of hyperthermia-based interventions.

Intrinsic photothermal MOFs harness the interplay between metal nodes and organic ligands to mediate energy transfer and electronic excitation [164]. This intrinsic mechanism affords a minimalist yet highly efficient thermal response, establishing a robust foundation for PTT while providing a versatile scaffold for integration with additional therapeutic modalities. Wang et al. developed core-shell Prussian Blue@MIL-100(Fe) dual-MOF nanoparticles designed for synergistic chemo-photothermal cancer therapy. The inner Prussian Blue (PB) nanocubes acted as the primary photothermal agent due to their strong and broad absorption in the NIR region, while the outer MIL-100(Fe) shell provided high surface area and mesoporous channels for efficient drug loading and pH-responsive release of artemisinin (ART). Upon 808 nm laser irradiation, the d-MOFs demonstrated rapid and concentration-dependent temperature elevation, confirming efficient photothermal conversion [165]. Zhang et al. developed spindle-like Janus nanomotors (Pt/FePc@Mn-MOF) integrating Mn-MOF, FePc nanozymes, and Pt nanoparticles for CT imaging-guided synergistic PTT-CDT. The Mn-MOF served as a porous backbone for loading FePc, which acts as both a photothermal agent and a catalyst for ROS generation. Pt nanoparticles were selectively grown on one side of the FePc@Mn-MOF to form an asymmetric Janus structure, enabling dual-source propulsion under H_2O_2 and NIR light, thereby enhancing tumor penetration and intracellular uptake. The nanomotors exhibited broad NIR absorption and high photothermal conversion efficiency. The incorporation of FePc within the Mn-MOF pores not only facilitated effective NIR light absorption but also enhanced local thermal gradients to induce self-thermophoretic motion, amplifying PTT effects. The Janus architecture, combined with dual chemical/NIR propulsion, significantly increased tumor accumulation and tissue penetration, promoting almost complete apoptosis and thermal ablation of cancer cells in vitro [166]. Composite photothermal MOFs achieve enhanced thermal conversion by incorporating exogenous functional entities within their pores or on their surfaces, enabling synergistic integration of photothermal effects with chemotherapeutic or photosensitizing agents [167]. Confined loading of photothermal or MW sensitizers improves energy absorption efficiency, prevents aggregation-induced activity loss or photobleaching, and improves circulation stability and tumor-site retention. Simultaneous incorporation of chemotherapeutic agents enables heat-triggered drug release, thereby promoting synergistic effects in PTT–CT or PTT–CDT. Wang et al. developed a core–shell CuS@Fe-MOF nanoplatform for MRI-guided PTT–CT. Hexagonal CuS nanosheets served as the photothermal core, around which an Fe-MOF shell was grown *in situ* via co-precipitation and assembly. DOX was loaded into the shell, and a lipid layer was applied to enhance aqueous dispersibility. The CuS core exhibited strong NIR absorption, with localized surface plasmon resonance providing efficient photothermal conversion. The Fe-MOF shell afforded pH-responsive drug release and T_2-weighted MRI functionality, integrating photothermal conversion, responsive CT, and imaging guidance within a single platform (Figure 7a) [168]. Wei et al. designed a degradable core–shell MOF nanoplatform (PAZDH), for photothermally enhanced CT–CDT. A ZIF-8 core served as a pH-responsive MOF, loading green-synthesized Bio-Ag nanoparticles, and was coated with polydopamine (PDA) to enable NIR photothermal conversion. Doxorubicin was loaded via π–π interactions, and hyaluronic acid modification facilitated CD44-mediated tumor targeting. The PDA layer markedly increased NIR absorption, producing concentration-dependent heating under 808 nm irradiation. Photothermal heating also accelerated ZIF-8 degradation and DOX release, while enhancing Bio-Ag-mediated Fenton-like reactions, thereby integrating thermal conversion, stimulus-responsive drugs delivery, CT, and CDT within a single intelligent system (Figure 7b) [169]. Zhu et al.

developed a MOF-based photothermal cascade nanoplatform (PUPG) to improve photothermal efficacy and overcome tumor thermotolerance. Pt nanoparticles were synthesized *in situ* within UiO-66-NH_2 pores, exploiting plasmonic resonance for efficient and stable NIR photothermal conversion. The MOF confinement mitigated Pt aggregation and thermal deformation, enhancing photothermal stability. Surface-grafted thermoresponsive PNIPAAm, loaded with the HSP90 inhibitor geldanamycin (GA), underwent conformational change under irradiation, triggering on-demand GA release to block HSP90-mediated thermal protection pathways, thus amplifying photothermal efficacy. This design demonstrated that MOFs can function both as photothermal carriers and as platforms for synchronized thermal conversion, heat-triggered release, and thermotolerance inhibition (Figure 7c) [170]. MOF-derived materials, generated via carbonization, oxidation, or pyrolysis, yield porous carbon, metal oxides, or metal–carbon composites with enhanced light absorption and thermal stability [171]. Surface modification further enables targeted delivery, integrating chemotherapeutic or immunomodulatory payloads with photothermal functionality, providing a robust platform for controlled mild PTT of deep-seated tumors.

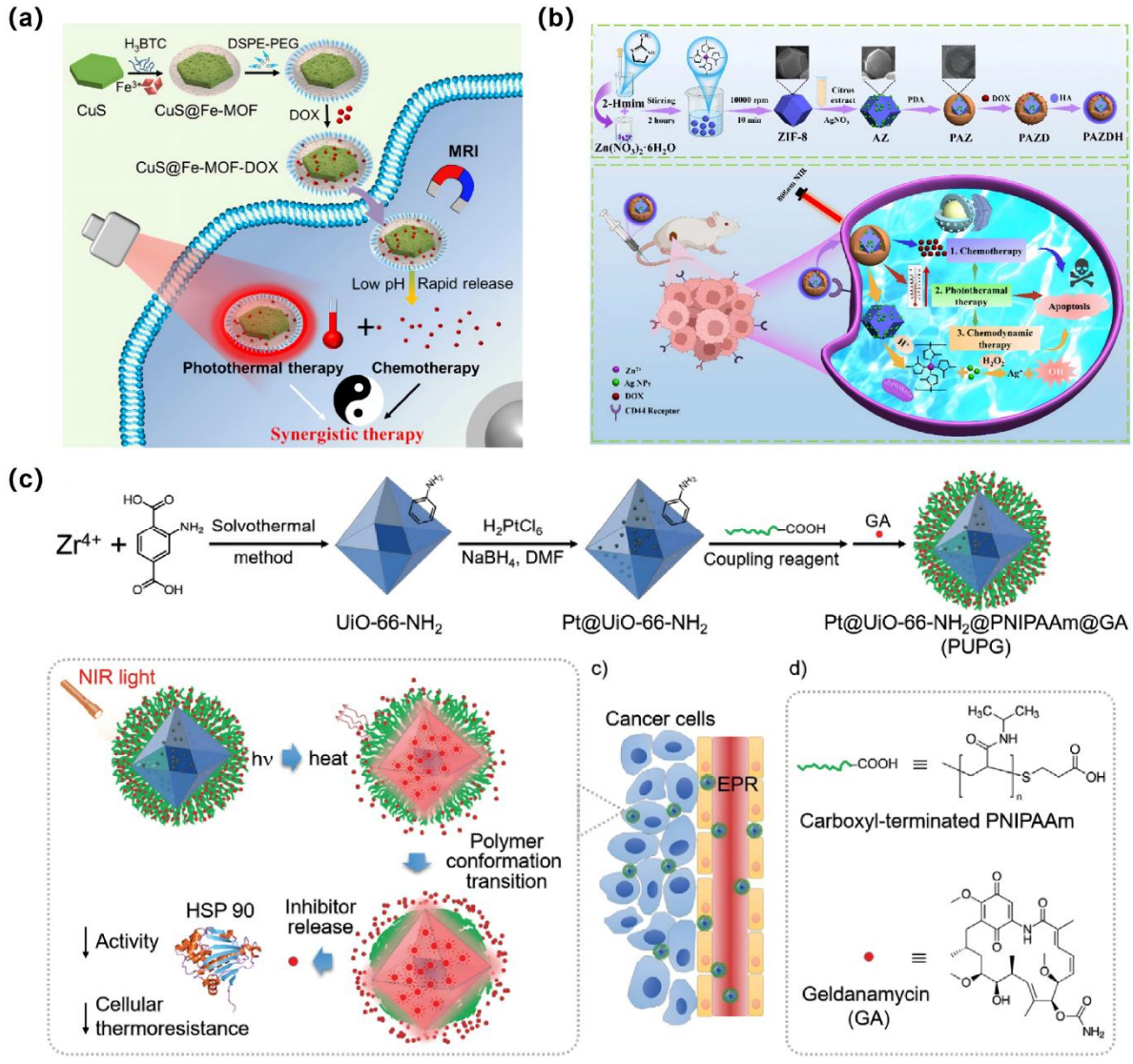

Figure 7. Representative MOF-based photothermal platforms designed for imaging guidance, chemotherapy sensitization, chemodynamic amplification, and thermoresistance suppression. (**a**) CuS@Fe-MOF combines a CuS photothermal core with a Fe-MOF shell for DOX loading, acid-responsive release, and MRI-guided PTT [168], Copyright 2020, Elsevier; (**b**) PAZDH integrates PDA-mediated photothermal heating with DOX delivery and Bio-Ag-catalyzed chemodynamic activity for enhanced combination therapy [169], Copyright 2025, Elsevier; (**c**) PUPG stabilizes Pt nanoparticles within UiO-66-NH2 and couples NIR-triggered heating with thermoresponsive GA release to inhibit HSP90-associated thermoresistance [170], Copyright 2022, WILEY.

MOF-based platforms for PTT offer not only efficient heat generation but also the potential for synergistic integration with other therapeutic modalities. The synergistic effect of MOF-based PTT arises from an integrated therapeutic cascade rather than from local hyperthermia alone. In this process, heat generation is mechanistically coupled with ROS amplification, stimuli-responsive drug release, TME remodeling, and immune activation [172]. Local temperature elevation can accelerate Fe, Cu, or Mn-mediated Fenton and Fenton-like reactions, thereby promoting the conversion of endogenous H_2O_2 into highly reactive ·OH. Meanwhile, metal ions released from MOF frameworks can deplete intracellular GSH and impair GPX4-related antioxidant defense, reducing the capacity of tumor cells to neutralize oxidative stress. Therefore, when PTT is combined with CDT or PDT, the thermal effect not only produces direct cytotoxic injury but also amplifies oxidative damage by enhancing ROS generation, weakening antioxidant buffering, and promoting lipid peroxidation [173]. Photothermal heating also provides a spatiotemporal trigger for synchronized drug release and therapeutic activation. Compared with conventional drug delivery, heat-triggered release allows therapeutic agents to be liberated preferentially within the heated tumor region, thereby increasing local drug exposure while limiting systemic toxicity. The heat-induced increases in cell membrane permeability and tumor vascular permeability can further facilitate drug penetration and intracellular accumulation [174]. In addition, MOF-mediated PTT can contribute to antitumor immune regulation through the induction of immunogenic cell death. Moderate thermal injury and ROS accumulation can promote the exposure or release of damage-associated molecular patterns, including calreticulin exposure, ATP secretion, HMGB1 release, and HSP expression. These signals enhance dendritic-cell antigen uptake and presentation, thereby facilitating T-cell priming and immune-cell infiltration into tumor tissue [175]. This mechanism is particularly relevant for mild PTT, where heat alone may be insufficient to eradicate tumor cells and may instead induce HSP70/HSP90-associated thermotolerance. By incorporating ROS amplification, HSP inhibition, GSH depletion, or immune activation into MOF-based platforms, sublethal thermal stress can be converted into stronger oxidative damage and antitumor immune responses, thereby improving local tumor control and reducing the risk of recurrence and metastasis [176]. Wu et al. employed MIL-100(Fe) as a host to encapsulate the plant-derived photosensitizer hypocrellin B (HB), further functionalizing the platform with either hyaluronic acid (HA) or RGD peptide to produce MHB-HA and MHB-RGD nanosystems for targeted multimodal phototherapy. The porous structure of MOFs enabled high loading efficiency of HB, while HA and RGD modification enhanced selective targeting toward CD44-overexpressing tumor cells and αvβ3 integrin-positive cells, respectively. HB conferred strong photothermal conversion, maintaining stability over repeated heating–cooling cycles. Concurrently, HB-generated $^1O_2$ under irradiation facilitated PDT, and MIL-100(Fe)-released Fe^{3+}/Fe^{2+} in the acidic TME catalyzed Fenton reactions to produce ·OH for CDT. This design demonstrated the capacity of MOFs to integrate PTT, PDT, CDT, and targeted delivery within a single platform, thereby maximizing tumor cell killing efficiency (Figure 8a) [177]. Li et al. introduced NIR phthalocyanine dye (Cy) into ZIF-8 through a one-step encapsulation process, constructing Cy@ZIF-8 nanoparticles for NIR imaging-guided PTT. The porous MOF framework improved Cy solubility, photostability, and cellular uptake, while pH-responsive degradation enabled accelerated NIR dye release in the acidic tumor microenvironment. Cy@ZIF-8 exhibited robust NIR fluorescence, allowing *in vivo* tracking of tumor accumulation and precise temporal control of photothermal activation. Encapsulation within ZIF-8 mitigated the limitations of free organic photothermal agents, including low stability, poor solubility, and rapid clearance, while simultaneously integrating photothermal conversion, stimulus-responsive release, and imaging functionality within a single MOF platform (Figure 8b) [178]. In strategies targeting ferroptosis or cuproptosis, hyperthermia can further amplify lipid peroxidation, while MOF-released metal ions catalyze ROS generation, producing synergistic enhancement between thermal stress and cell death pathways. Wang et al. developed a copper-doped MOF nanoplatform (DCZP), for GSH-depletion-enhanced combinatorial therapy, integrating CT, PTT, and CDT. The Cu-doped ZIF-8 served as a pH-responsive carrier for DOX, while the PDA coating endowed NIR photothermal conversion capability. In acidic tumor microenvironments, DCZP degraded to release DOX and Cu^{2+}, with Cu^{2+} reduced by intracellular GSH to Cu^+, thereby depleting GSH and disrupting redox homeostasis. Cu^+ catalyzed H_2O_2 via Fenton-like reactions to produce ·OH, while local photothermal heating accelerated both DOX release and ROS generation, achieving amplified tumor cell damage (Figure 8c) [179].

Overall, the application of MOF-based materials in PTT exemplifies a high degree of coordination among structural design, energy conversion, functional integration, and combinatorial treatment. Rational design of intrinsic, composite, and MOF-derived systems enables efficient local heating, ROS generation, controlled drug release, and imaging-guided monitoring, providing a robust material foundation for mild hyperthermia and multimodal therapeutic strategies.

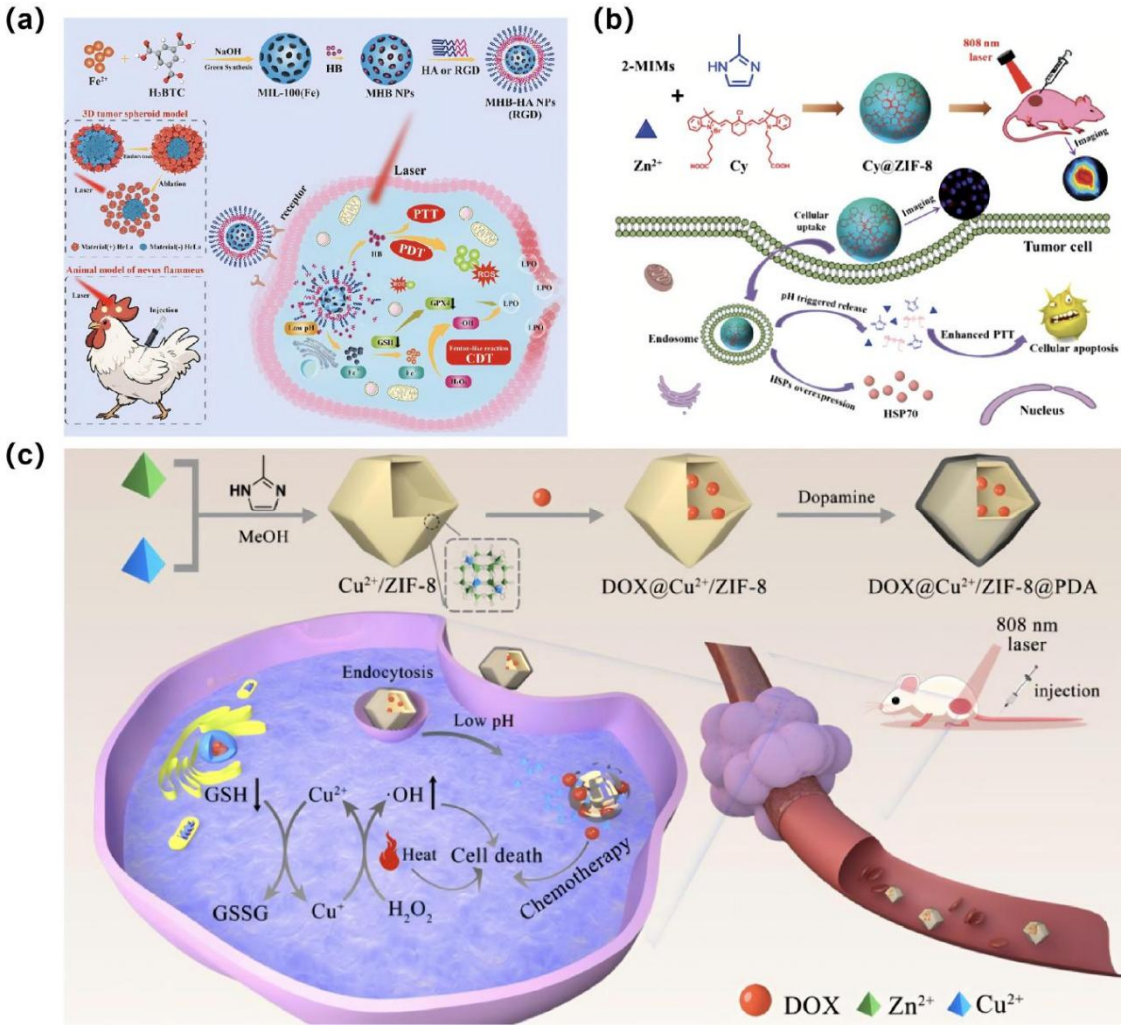

Figure 8. MOF-based photothermal platforms integrating light-responsive components with targeted delivery, tumor-responsive release, catalytic therapy, chemotherapy, and imaging guidance. (**a**) MHB-HA/RGD couples hypocrellin B-mediated PTT/PDT with Fe-catalyzed CDT in a targeted MIL-100(Fe) system [177], Copyright 2025, Elsevier; (**b**) Cy@ZIF-8 improves cyanine dye delivery and stability for NIR imaging-guided PTT [178], Copyright 2018, Royal Society of Chemistry; (**c**) DOX@Cu^{2+}/ZIF-8@PDA combines PDA-mediated heating with DOX release, GSH depletion, and Cu-driven CDT [179], Copyright 2022, Elsevier.

4.2. MWH

MWH employs electromagnetic waves to generate localized heating within tumor tissues, leveraging the thermal effects of microwaves to achieve spatially precise ablation and cytotoxicity [180]. Compared with other energy modalities, MW offer superior tissue penetration and reduced dependence on local water content, enabling effective heat delivery to deep-seated tumors and maintaining thermal stability in hydrated tissues [181]. The hierarchical porosity and high surface area of MOFs enhance multiple reflections and scattering of MW energy within the material, increasing local energy deposition. Simultaneously, interfacial polarization between metal nodes and organic ligands facilitates efficient conversion of MW energy into heat via combined dielectric and magnetic losses, resulting in controllable local hyperthermia [182].

Owing to the high surface area and precisely controllable porosity, MOFs provide an effective framework for confining endogenous ions present in the TME or incorporating exogenous ionic species, such as ionic liquids, within the internal pore space [183]. Compared with conventional ionic MW sensitizers, the porous structure of MOFs restricts ion mobility, preventing diffusion into surrounding healthy tissues, which minimizes off-target toxicity while enhancing ion utilization and thermal conversion efficiency. Qin et al. employed an *in situ* doping strategy to construct Mn-doped Ti-based MOF nanosheets (Mn-Ti MOFs@PEG) for MRI-guided MWH combined with MWDT. The Ti-based framework, featuring hierarchical porosity and high surface area, promoted high-frequency collisions of confined ions under MW irradiation, resulting in efficient conversion of electromagnetic energy into localized heat. Mn incorporation introduced structural defects and reduced the bandgap of Ti-MOF,

facilitating electron–hole separation and $^1O_2$ generation at low-power MW irradiation, thereby amplifying MWDT. In addition, Mn-doped MOFs exhibited T_1-weighted MRI contrast, enabling visualization of intratumoral accumulation and guiding subsequent MW treatment, highlighting the potential of Mn-Ti MOFs for imaging-guided MWH and MWDT (Figure 9a) [184]. The coordination of metal nodes or clusters with organic ligands imparts MOFs with distinctive dielectric and magnetic properties, allowing efficient MW absorption via combined dielectric and magnetic losses [185]. Electronic transitions in metal centers, together with charge transfer between ligands and metal ions, generate polarization centers that undergo electronic, ionic, and interfacial polarization under alternating MW fields, dissipating energy as heat through relaxation processes [186]. For MOFs containing magnetic ions such as Fe or Mn, domain reorientation, natural resonance, and eddy current phenomena contribute to hysteresis and magnetic losses, further converting electromagnetic energy into heat [187]. Fu et al. synthesized Mn-ZrMOF NCs via a one-step hydrothermal method for synergistic MWH and MWDT. Under MW exposure, these nanocubes confined ions within the pores, promoting inelastic collisions between ions and the flexible MOF framework, which efficiently converts MW energy into localized heat. Mn doping additionally provided peroxidase-like catalytic activity, enabling H_2O_2-mediated ·OH generation and enhancing the therapeutic efficacy of MWDT. *In vivo* experiments confirmed that Mn-ZrMOF NCs combined with MW irradiation significantly increased intratumoral temperature and, through the synergy of thermal and ROS-mediated cytotoxicity, suppressed tumor growth (Figure 9b) [188]. Wang et al. developed a TME-responsive nanoregulator CMALRH, designed to enhance MDT through a multi-pronged ROS amplification strategy. The CoMnMOF framework acted as a MW sensitizer, leveraging its porous structure to confine metal ions and polar molecules, thereby enhancing local heating under MW irradiation. The platform also incorporated a GSH-responsive mechanism, in which disulfide bonds reacted with overexpressed GSH in tumor cells, facilitating GSH depletion and promoting intracellular ROS accumulation. Simultaneously, the release of Co^{2+} and Mn^{2+} ions catalyzed the decomposition of H_2O_2 to O_2, alleviating tumor hypoxia and further amplifying ROS generation. The loaded Apatinib additionally inhibited VEGF expression, providing a combined effect of hypoxia relief, antioxidant depletion, and ROS amplification [189]. Precise tuning of metal nodes, ligand structures, and pore structure allows MOFs to modulate dielectric and magnetic loss pathways, thereby maximizing MW energy dissipation and thermal conversion efficiency, which in turn enhances the performance of MOF-based MWH platforms.

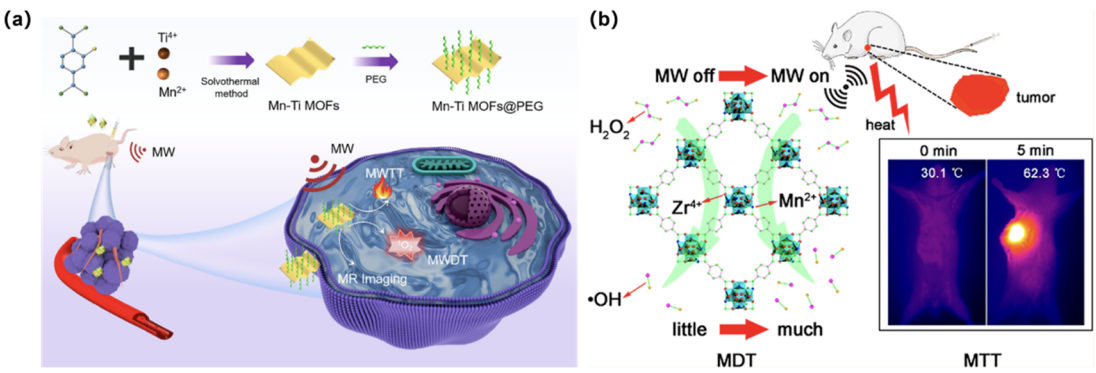

Figure 9. Mn-doped MOF platforms for microwave-responsive thermal and radical-based tumor therapy. (**a**) Mn-Ti MOFs@PEG combine microwave-triggered heating, $^1O_2$ production, and T_1 MRI guidance through Mn-regulated Ti-MOF nanosheets [184], Copyright 2023, Elsevier; (**b**) Mn-ZrMOF NCs promote MW energy dissipation and Mn-assisted ·OH generation for synergistic MWH and MDT [188], Copyright 2017, ACS Publications.

The porous structure of MOFs enables efficient sequestration of endogenous ions within the TME or encapsulation of exogenous ionic species within confined pore networks. Confinement within nanoscale channels enhances the collision frequency of ions or polar molecules, thereby facilitating the efficient conversion of MW energy into localized heat [190]. Li et al. developed a MOF@COF nanocapsule, BMCAP, for combinatorial MWH, MWDT, and anti-angiogenic treatment of colorectal cancer. The platform employed a Bi–Mn porphyrinic MOF core in which Bi^{3+}, Mn^{2+}, and TCPP constituted the microwave-responsive unit. Under MW irradiation, the porous structure enabled ion confinement that amplifies local heating, while Mn active sites and the porphyrin framework facilitated electron–hole separation and $^1O_2$ generation for MWDT. A COF shell stabilizes the nanocapsule, enhanced MW sensitization, promoted ROS production, and allowed π–π-mediated loading of the anti-angiogenic agent apatinib. Consequently, MW exposure triggered simultaneous localized heating, ROS generation, and drugs release, achieving synergistic tumor inhibition through combined MWH, MWDT, and VEGF downregulation (Figure 10a) [191]. The tunable metal nodes and ligand frameworks of MOFs endow them

with versatile physicochemical and magnetic properties. Zhou et al. reported a mitochondria-targeted ZrMOF-PEG-TPP@DOX platform for enhanced MWH. The high surface area and rich microporosity of the ZrMOF nanocubes promoted high-frequency collisions of surrounding ions under MW irradiation, facilitating efficient conversion of electromagnetic energy into localized heat. The system achieved temperatures of approximately 54.5 °C in DMEM without the need for exogenous ionic liquids. PEGylation improved colloidal stability, while TPP functionalization enabled mitochondrial targeting, and DOX loading provided combinatorial CT. Enrichment of the nanoplatform within mitochondria enhanced intracellular utilization of the MW sensitizer, increased local thermal deposition, and improved therapeutic efficacy, representing a rational design for deep-tumor MWH (Figure 10b) [192]. Compared with conventional inorganic microwave-responsive agents, MOFs may offer superior biocompatibility due to their organic ligands and degradability under acidic or enzymatic conditions, allowing safe clearance of degradation products and mitigating long-term toxicity [193]. Surface functionalization further enhances biocompatibility, *in vivo* stability, and tumor-targeting capability, facilitating clinical applicability [194]. MOFs can also co-load chemotherapeutics, immunomodulators, or photosensitizers, enabling synergistic integration of MWH with other therapeutic modalities [195]. Additionally, some MOF platforms possess intrinsic imaging capabilities, allowing real-time visualization of nanoparticle distribution and treatment monitoring, thereby supporting precision-guided MWH [196]. Chen et al. demonstrated a logic-gated theranostic platform, APGS NCs, which co-encapsulates $HAuCl_4$, the phase-change material 1-tetradecanol, and Gd-MOF within dendritic mesoporous SiO_2 nanoparticles. The inclusion of Gd-MOF significantly enhanced microwave-induced heating, while the dendritic pore structure accommodated abundant ions, promoting high-frequency motion and collisions under MW fields to achieve efficient energy dissipation and localized thermal conversion. MW irradiation combined with high intracellular GSH triggered *in situ* reduction of $HAuCl_4$ to fluorescent Au clusters, translating thermal damage into an imaging signal. This approach highlighted the capacity of MOF-based platforms to integrate MW energy conversion with stimulus-responsive imaging, providing a framework for real-time monitoring and feedback in precision MWH (Figure 10c) [197].

MWH can also be exploited to regulate drug release from MOF-based delivery systems. Owing to the superior tissue penetration of MW, this modality is particularly suitable for localized heating of deep-seated tumors, enabling chemotherapeutic agents confined within MOF pores to be released in synchrony with MW irradiation. Microwave-induced local heating can accelerate framework loosening, increase shell permeability, or trigger the melting of phase-change components, thereby aligning drug liberation with the thermal treatment [198]. In addition, the elevated temperature can improve tumor blood perfusion and enhance cellular membrane permeability, facilitating drug diffusion and intracellular uptake. Zhao et al. developed a Gd/Eu bimetallic MOF nanoplatform (GEMT) for combinatorial MWH and hypoxia-activated CT in breast cancer. The platform employed Gd^{3+} and Eu^{3+} as metal nodes to construct GdEuMOF (GEM) via a solvothermal approach, subsequently loading the hypoxia-activated prodrug tirapazamine (TPZ). GEM exhibited efficient MW sensitization, with the porous architecture enabling ion confinement that amplified local energy dissipation and elevates tumor temperature. Microwave-induced perturbation of blood flow and microthrombosis established an initial hypoxic state, while Eu^{2+} release under weakly acidic conditions further consumes residual oxygen, generating a secondary hypoxic environment. This two-stage hypoxia amplification facilitates TPZ reduction and activation, producing highly cytotoxic radicals and enhancing CT efficacy, thereby achieving synergistic tumor inhibition through coordinated MW sensitization, hypoxia modulation, and prodrug activation (Figure 11a) [199]. Transition-metal nodes within MOFs can catalyze the generation of ROS, including ·OH and $^1O_2$, under MW irradiation. These ROS act synergistically with thermal effects, damaging cellular membranes, proteins, and DNA, thereby enhancing apoptosis [200]. Ma et al. reported a biomimetic microwave-sensitized platform (SNAP/MOF@HCM) for enhanced hepatocellular carcinoma ablation. The system comprised a ZIF-8 core loaded with the NO donor SNAP, which was coated with a hybrid membrane derived from tumor cells and cancer-associated fibroblasts (CAFs). The high surface area and porosity of ZIF-8 concentrated ions within the channels, which promoted high-frequency motion and inelastic collisions under MW irradiation, resulting in efficient local heat generation with good thermal stability. The hybrid membrane provided dual targeting toward tumor cells and CAFs, which improved intratumoral accumulation and cellular uptake. MW and GSH co-stimulation triggered NO release from SNAP, which suppressed CAF activation, reduced collagen and fibronectin deposition, and mitigated the dense extracellular matrix barrier, thereby enhancing intratumoral heat conduction and nanoparticle penetration. Concurrently, Zn^{2+} released from ZIF-8 induced Fenton-like reactions generating ·OH, which, together with NO, amplified oxidative damage, induced apoptosis, and promoted immunogenic cell death, ultimately improving the efficacy of MWH (Figure 11b) [201]. Under mild hyperthermia conditions, MOF platforms can simultaneously coordinate drug release and MW sensitization, integrating thermal effects, ROS production, CT, and immune activation [202]. Zhao et al. constructed a lanthanide-based EuMOF@ZIF/AP-PEG (EZAP) nanocomposite for

combinatorial MWH, CT, and fluorescence imaging in hepatocellular carcinoma. EuMOF served as the microwave-sensitizing and fluorescent core, and a ZIF shell enhanced stability under physiological conditions while providing increased drug-loading capacity for apatinib. PEGylation further improved systemic circulation. *In vivo* studies demonstrated that EZAP, combined with MW exposure, significantly increased intratumoral temperature and, through synergistic MWH and apatinib CT, achieved a tumor inhibition rate of 98.5%. The platform thus exemplified the integration of MW sensitization, targeted drug delivery, and imaging-guided therapy within a single MOF-based system, providing a representative strategy for precision MWH (Figure 11c) [203]. Guo et al. developed a metal-organic framework nanoamplifier (GCZMT) for MW thermal-immunotherapy, exemplifying the use of MOFs to enhance microwave-induced thermal conversion and therapeutic efficacy. In this design, the ZrMOF-NH_2 framework encapsulated both the NO donor CSNO and the HSP70 activator teprenone (GGA), while the channels were blocked with a temperature-responsive L-menthol (LM) switch and functionalized with a mitochondria-targeting ligand (TPP). Upon MW irradiation, the temperature rise triggered LM melting, releasing CSNO and GGA. CSNO decomposition produced NO in mitochondria, causing mitochondrial damage and oxidative stress, while GGA and NO synergistically upregulated HSP70 expression. This programmed HSP70 upregulation enhanced cytotoxic $CD4^+$ and $CD8^+$ T cell responses, combining thermal ablation with immune activation [204].

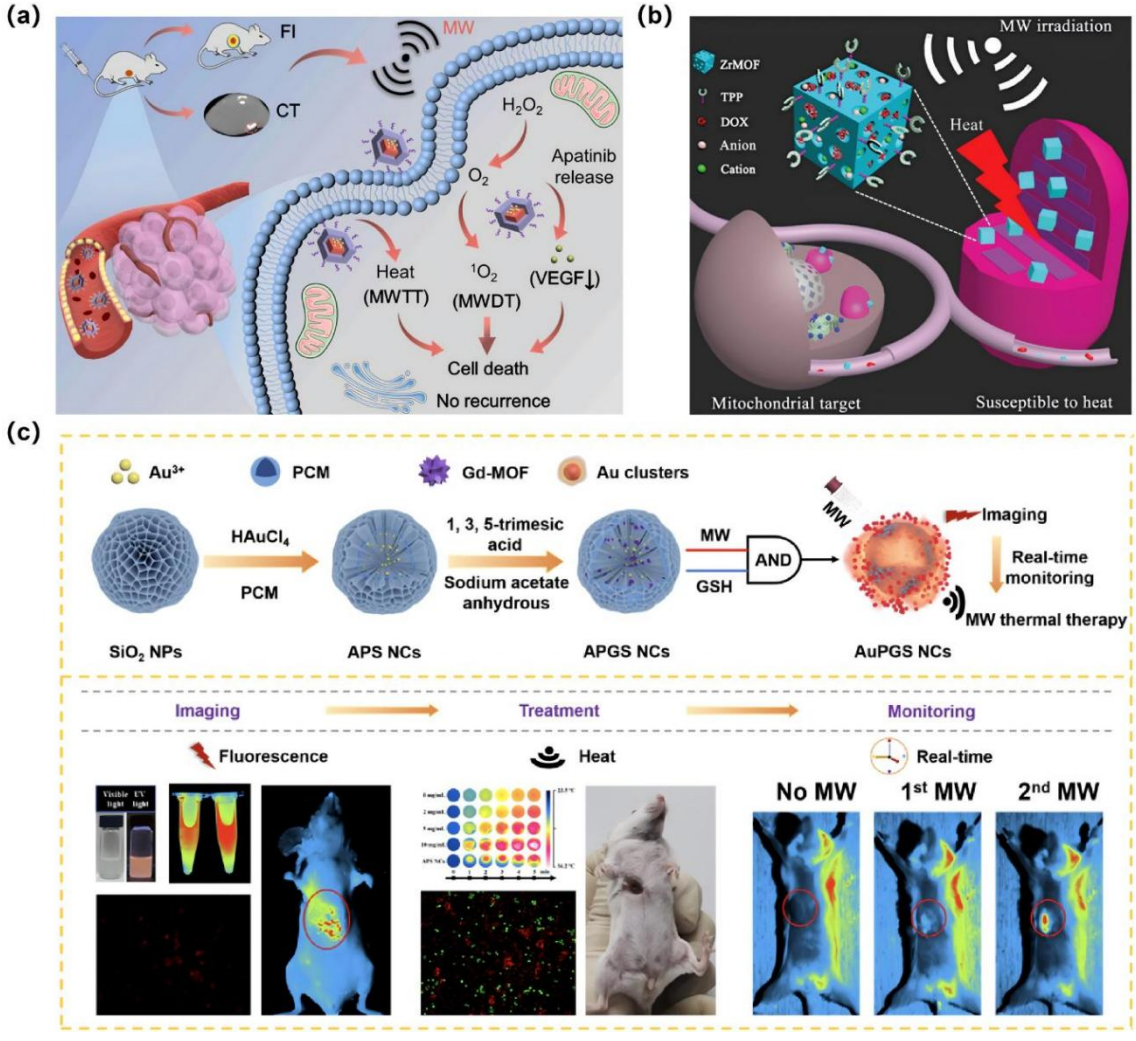

Figure 10. MOF-based MWH platforms integrating microwave sensitization with anti-recurrence therapy, mitochondrial targeting, and treatment-feedback imaging. (**a**) BMCAP couples MOF@COF-assisted MW heating with microwave-induced $^1O_2$ generation and apatinib delivery for anti-angiogenic tumor suppression [191], Copyright 2022, Elsevier; (**b**) ZrMOF-PEG-TPP@DOX directs MW sensitizers toward mitochondria to enhance heat susceptibility and improve microwave-mediated tumor ablation [192], Copyright 2018, RSC Publishing.; (**c**) APGS NCs combine Gd-MOF-mediated MW heating with MW/GSH-activated fluorescence, enabling real-time visualization of the thermal treatment process [197], Copyright 2023, Elsevier.

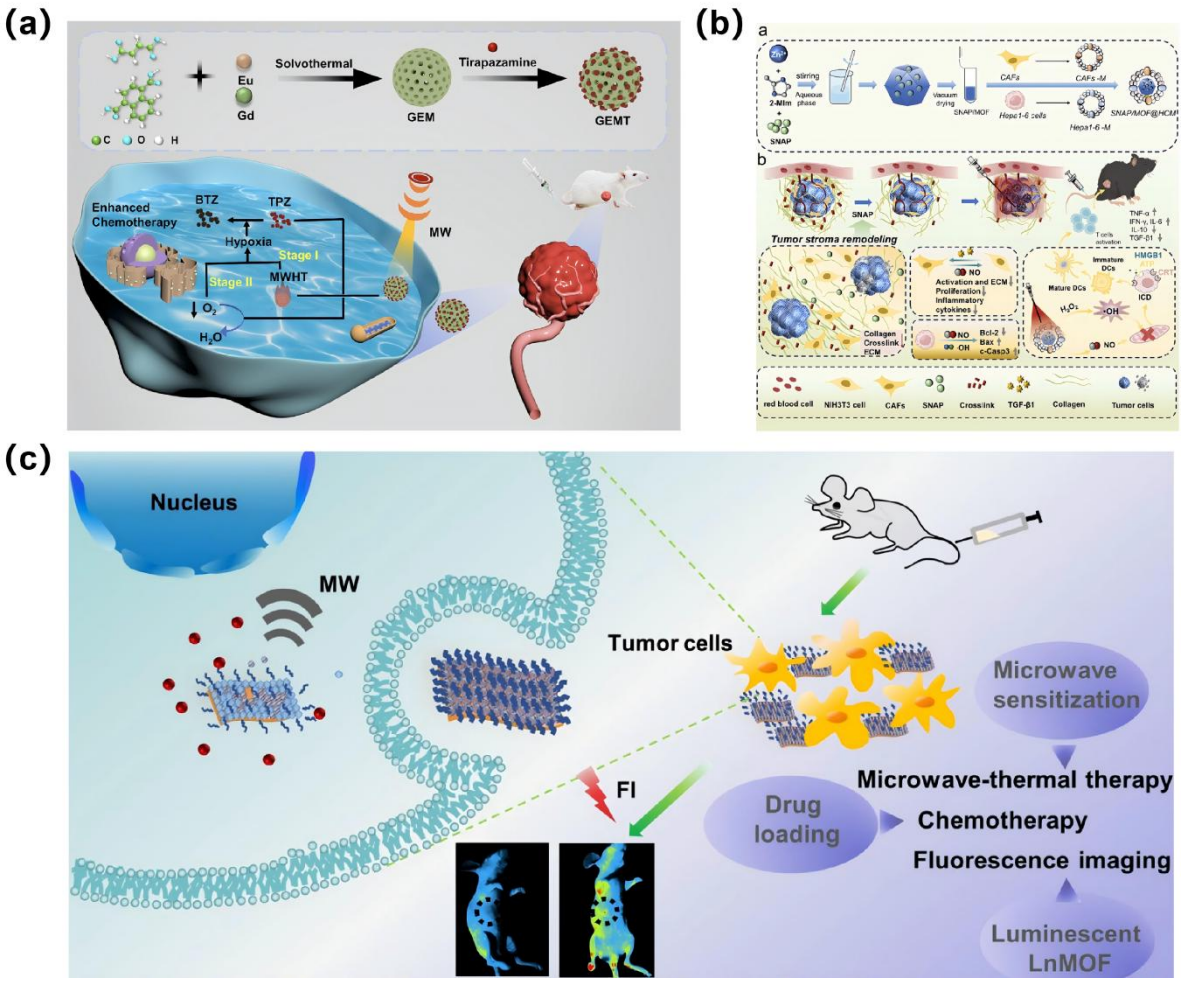

Figure 11. MOF-enabled MW therapeutic platforms combining energy sensitization with hypoxia modulation, stromal remodeling, CT, and fluorescence-guided intervention. (**a**) GEMT enhances MWH and activates CT through sequential hypoxia amplification mediated by Gd/Eu-MOF [199], Copyright 2024, Elsevier; (**b**) SNAP/MOF@HCM improves MW ablation by coupling NO-assisted stromal remodeling with oxidative/nitrosative stress and immune activation [201], Copyright 2026, Elsevier; (**c**) EZAP integrates EuMOF-mediated MW sensitization with apatinib delivery and fluorescence imaging for image-guided MWH-CT [203], Copyright 2022, Spring Nature.

Compared with PTT, the synergistic mechanisms of MOF-mediated MWH are more closely associated with deep-tissue energy deposition, enhanced dielectric or magnetic dissipation, and microwave-amplified ROS generation. Under MW irradiation, metal nodes, polar linkers, defect sites, and loaded ions within MOF frameworks can contribute to dipolar rotation, ionic conduction, interfacial polarization, and magnetic loss, thereby converting MW energy into localized heat [205]. This process not only elevates the temperature within the tumor region but also promotes metal-node-mediated catalytic reactions. In addition, microwave-induced thermal stress can disrupt mitochondrial membrane potential and cellular redox homeostasis, allowing catalytically generated ROS to synergize with endogenous oxidative stress. This convergence of oxidative insults can intensify DNA damage, lipid peroxidation, and apoptotic cell death [206]. From an immunomodulatory perspective, MOF-based MWH also holds potential for inducing immunogenic cell death and remodeling the tumor immune microenvironment [207]. Compared with surface-limited PTT, MWH is better suited for deep-seated solid tumors, where *in situ* antigen release may convert tumor tissue into an endogenous source of tumor-associated antigens.

Overall, MOF-based materials have emerged as highly promising microwave-sensitizing agents due to their tunable porous architectures, abundant active sites, biocompatibility, and capacity for multifunctional integration. Through the synergistic effects of ion confinement and electromagnetic energy dissipation, these platforms enhanced the precision and efficacy of MWH, offering novel strategies to address challenges in clinical MWH applications.

4.3. Enhanced Performance of MOF Platforms over Conventional Agents

Although MOF-based materials have demonstrated considerable potential for multifunctional integration in tumor hyperthermia, their advantages and limitations can be more clearly defined when evaluated against conventional thermal nanoplatforms. Representative photothermal nanomaterials include gold nanorods, black phosphorus, indocyanine green, and copper sulfides [208]. These materials typically exhibit strong near-infrared absorption and efficient photothermal conversion, enabling rapid local temperature elevation. Nevertheless, many conventional photothermal agents remain functionally limited, with restricted drug-loading capacity and limited capability for stimulus-responsive therapeutic integration. In addition, some systems are associated with *in vivo* retention, insufficient photostability, aggregation-induced quenching, or incompletely defined metabolic pathways [209]. Therefore, although these materials are highly effective for single-mode photothermal conversion, the construction of multimodal therapeutic platforms often requires additional carriers, surface engineering, or auxiliary functional components. By contrast, the major strength of MOF-based photothermal platforms lies in the structural programmability and functional integration capacity. MOFs can generate photothermal effects through metal nodes, π-conjugated linkers, defect sites, or MOF-derived carbon structures, while their ordered pore networks provide accessible compartments for chemotherapeutic agents, photosensitizers, or thermoresistance inhibitors. These drugs can be released in response to tumor-associated or externally applied triggers, including acidic pH, GSH, enzymes, and heat. Compared with conventional photothermal agents, MOFs are therefore better suited for integrating PTT with CT, CDT, and immune modulation within a single material platform. In addition, the confinement effect of MOF pores can improve the dispersion of photosensitizers or photothermal agents, reducing dye aggregation, photobleaching, and nanoparticle clustering, thereby improving therapeutic stability and controllability. However, the photothermal performance of MOFs is highly dependent on framework composition and post-synthetic engineering. Some intrinsic MOFs exhibit limited near-infrared absorption and therefore require linker engineering, metal doping, exogenous photothermal-agent incorporation, or derivatization to achieve sufficient photothermal efficacy.

In MWH, conventional microwave-responsive materials mainly include metal oxides, ferrites, and selected semiconductor nanomaterials. These materials can convert MW energy into heat through dielectric loss, magnetic loss, ionic conduction, or interfacial polarization, thereby offering advantages for deep-tissue tumor treatment [210]. Nevertheless, conventional MW sensitizers often suffer from poor dispersibility, heterogeneous thermal-field distribution, limited tumor selectivity, and insufficient capability for synchronized drug delivery [211]. Although some inorganic materials exhibit strong microwave absorption, the relatively limited surface-engineering capacity often restricts them to a narrow range of therapeutic functions. MOF-based MWH platforms provide distinct advantages in both microwave-responsive mechanisms and combination-therapy design. Their porous frameworks can confine the motion of ions, water molecules, and polar species, promoting high-frequency vibration, dipolar rotation, and polarization relaxation under MW irradiation, thereby enhancing localized energy deposition. In addition, metal nodes, metal-linker interfaces, crystallographic defects, and multimetallic architectures can introduce interfacial polarization, conductive loss, or magnetic loss, further improving microwave-to-heat conversion. The ordered pore structure of MOFs also enables the incorporation of chemotherapeutic agents, immunomodulators, or MW sensitizers, allowing microwave-induced heating to be coupled with drug release, ROS generation, and immune activation. Thus, compared with conventional microwave-responsive materials, MOFs are not merely MW energy transducers but multifunctional reaction platforms for deep-tumor combination therapy. However, the MW absorption capacity and thermal robustness are not necessarily superior to those of specifically engineered ferrites, carbon-based absorbers, or dielectric ceramics. Under high-power or prolonged MW exposure, framework stability, metal-ion release, and *in vivo* degradation behavior remain critical issues that require systematic evaluation.

Overall, conventional photothermal and microwave-responsive nanomaterials often show clear advantages in single-mode energy conversion because of their relatively simple structures and direct thermal-response mechanisms. In contrast, the primary strength of MOFs lies in their programmable framework chemistry, porous drug-loading capacity, catalytically active metal nodes, surface modifiability, and capacity for multimodal diagnostic and therapeutic integration. MOFs therefore should not be regarded solely as high-efficiency thermal transducers, but rather as versatile platforms for constructing integrated therapeutic systems.

5. Challenges and Perspectives

Despite the exceptional thermal responsiveness, multifunctional integration potential, and structural tunability of MOFs in PTT and MWH, the clinical translation remains constrained by multiple factors. Achieving precise thermal control in deep-seated tumors continues to limit treatment efficacy. Tumor heterogeneity and

dynamic blood perfusion result in spatially uneven energy deposition from MW or NIR irradiation, potentially causing subtherapeutic heating in target regions or excessive thermal exposure in adjacent normal tissues, thereby compromising safety and efficacy. Furthermore, tumor cells can develop adaptive thermotolerance over the course of treatment, including upregulation of heat shock proteins, enhancement of antioxidant defenses, and microenvironmental buffering, which may attenuate the effectiveness of monomodal hyperthermia. Consequently, single-mode thermal therapy alone is insufficient to achieve optimal antitumor outcomes, and integration with CT, PDT, or MWDT is necessary to realize synergistic therapeutic amplification.

Comprehensive characterization of MOF-based compounds is essential to assess the structural stability, degradation behavior, and long-term biocompatibility *in vivo*. Although MOFs undergo controlled disassembly under acidic or enzymatic conditions, the precise metabolic and excretion pathways remain insufficiently understood, raising concerns regarding potential tissue accumulation and chronic toxicity. Effective delivery to deep-seated tumors is further constrained by clearance through the mononuclear phagocyte system, necessitating optimization of surface engineering strategies, such as PEGylation, peptide conjugation, or biomimetic membrane coatings, to enhance circulation stability and active tumor targeting. In MWH, the efficiency of thermal sensitization is governed by a combination of ion confinement within MOF pores and dielectric and magnetic loss mechanisms. However, precise tuning of metal composition, ligand architecture, and pore dimensions to coordinate local thermal deposition with ROS generation remains a significant challenge. Integration of computational modeling, real-time thermal mapping, and imaging guidance may facilitate rational optimization of material structures and irradiation parameters, enabling highly controlled and spatially precise energy delivery. The therapeutic outcome of tumor hyperthermia is highly dependent on the local temperature range. Insufficient heating may fail to induce effective tumor-cell injury, whereas excessive temperature elevation can damage adjacent normal tissues, trigger inflammatory responses, or even cause irreversible necrosis [212]. Therefore, the design of MOF-based hyperthermia platforms should not focus exclusively on photothermal conversion efficiency or MW absorption capacity. Equal attention should be given to the dynamic regulation of heat generation, heat diffusion, and thermal dissipation. Precise thermal regulation requires optimization at both the material and treatment-protocol levels. At the material level, the thermal response of MOFs can be tuned by modulating metal nodes, linker structures, pore dimensions, and surface chemistry, allowing more predictable temperature elevation under defined light power or MW intensity [213]. Thermoresponsive polymers and phase-change materials can also be incorporated into MOF systems, enabling conformational changes, drug release, or heat-dissipation regulation once a predefined temperature threshold is reached. Such designs may provide a degree of adaptive thermal control [214]. In addition, external energy parameters, including power density, irradiation duration, and treatment area, require precise adjustment. Future studies should move beyond fixed-power and fixed-time treatment protocols and instead establish individualized thermal dose regimens based on tumor size, depth, blood perfusion, and intratumoral material accumulation. Real-time thermal monitoring is equally critical for improving the safety and controllability of hyperthermia. Many preclinical studies currently rely on infrared thermal imaging to monitor tumor surface temperature, but this approach cannot accurately capture intratumoral temperature or spatial thermal gradients in deep tissues. For clinical translation, more accurate thermometric strategies are required, including magnetic resonance thermometry, ultrasound thermometry, photoacoustic imaging, and implantable microscale temperature sensors [215]. MOFs are particularly attractive in this context because imaging components can be integrated into their framework or porous structure. For example, Mn, Gd, or Fe-based nodes, temperature-sensitive dyes, photoacoustic probes, or magnetic resonance-responsive components can be incorporated to enable temperature feedback and spatial localization during treatment.

Despite extensive exploration of multifunctional integration and combination therapy, clinical translation of MOF-based platforms continues to be limited by factors such as reproducibility across batches, scalable synthesis, predictable *in vivo* drug release kinetics, and compatibility with established therapeutic modalities. Future efforts should therefore prioritize systematic approaches to rational material design, precise thermal field modulation, optimization of multimodal therapy strategies, and rigorous long-term safety evaluation. By aligning structural, functional, and *in vivo* performance parameters, MOFs can be advanced into safe, effective, and controllable hyperthermia platforms suitable for minimally invasive cancer treatment. For clinical translation, MOF-based hyperthermia platforms must be evaluated not only as high-performance nanomaterials, but also as clinically deployable therapeutic systems. Their design should be matched to the intended treatment scenario. Because near-infrared irradiation has limited tissue penetration, photothermal MOF platforms are more appropriate for superficial tumors, surgically exposed lesions, or lesions accessible by fiber-optic delivery [216]. Microwave-responsive MOFs, by contrast, are more relevant to deep-seated solid tumors owing to the greater penetration of MW energy, although selective tumor accumulation, spatially confined energy deposition, and protection of adjacent normal tissues remain essential requirements [217]. Therefore, in vitro thermal conversion efficiency

alone is insufficient to define translational value. Tumor type, anatomical location, administration route, and compatibility with existing clinical heating devices should be considered from the early stage of material design. Manufacturing scalability and quality control represent equally important translational constraints. Many reported MOF-based hyperthermia systems depend on multistep synthesis, sequential drug loading, surface functionalization, or complex multicomponent assembly. For clinical development, platforms with well-defined composition, simplified synthesis, controllable structural parameters, and reproducible batch quality are likely to be more viable than highly complex systems built through excessive functional integration. A more standardized translational evaluation framework is also needed. Differences in power density, irradiation duration, administered dose, and tumor model currently limit direct comparison across studies. Future work should adopt more consistent animal models, harmonized thermal parameters, clinically relevant controls, and long-term outcome measures to improve reproducibility and clinical interpretability. Future development should therefore move away from indiscriminate functional stacking and toward clinically driven platform design, prioritizing clear composition, scalable manufacturing, validated safety, and compatibility with established hyperthermia equipment.

In addition, biosafety and *in vivo* metabolic behavior remain critical issues for the clinical translation of MOF-based hyperthermia platforms. These systems are typically composed of metal nodes, organic linkers, therapeutic drugs, and surface-modification layers, and may undergo circulation, tumor accumulation, cellular uptake, degradation, and excretion after administration. Accordingly, short-term cytotoxicity assays and H&E staining of major organs are insufficient to establish a comprehensive safety profile. Metal-ion release represents one of the major potential sources of toxicity. High-valence metal MOFs based on Zr, Ti, or Hf generally exhibit favorable structural stability, but excessive stability may prolong *in vivo* retention. Transition-metal MOFs containing Fe, Cu, or Mn can enhance Fenton-like reactions, GSH depletion, magnetic responsiveness, or MW sensitization, yet the released metal ions may induce nonspecific oxidative stress, inflammatory responses, or organ toxicity. A balance must therefore be established between therapeutic activity and metal-release safety, together with systematic assessment of dose-dependent toxicity for different metal nodes. The degradation pathways and long-term mechanisms of MOF-based materials also require further clarification. Premature degradation in the bloodstream may lead to drug leakage and off-target tissue injury, whereas excessive structural persistence may result in prolonged accumulation in organs such as the liver, spleen, or lung. These concerns are amplified for MOF-derived carbonaceous materials, metal sulfides, and metal/carbon hybrids, for which degradation, clearance, and residual retention may follow more complex pathways. Their *in vivo* fate should therefore be established through longitudinal biodistribution studies, elemental mapping and quantification, fecal and urinary clearance analysis, and comprehensive organ-function assessment. Immunological safety represents another critical dimension of translational evaluation. Following systemic administration, protein corona formation may reshape biodistribution, macrophage recognition, and complement activation [218]. Although cell-membrane camouflage, hyaluronic acid modification, and peptide conjugation can improve circulation persistence and tumor selectivity, these surface-engineering strategies may also introduce additional immunological variables, including anti-PEG responses, residual membrane-associated antigens, and immune activation after repeated dosing [219]. Accordingly, hemocompatibility, macrophage polarization, and complement activation should be incorporated into standardized safety-assessment frameworks.

Collectively, the tunable porosity, high density of metal–ligand interfaces, and versatile functionalization capabilities of MOFs provide a robust foundation for tumor hyperthermia applications. Nonetheless, ensuring precise energy deposition, effective integration with combinatorial therapies, targeted delivery, and comprehensive biocompatibility assessment is imperative to realize the full clinical potential of MOF-based hyperthermia systems.

6. Conclusions

Characterized by highly tunable three-dimensional porous structures, well-defined metal-organic interfaces, and versatile surface functionalization capabilities, MOFs have emerged as highly promising platforms for photothermal and microwave-mediated tumor hyperthermia. Intrinsic, composite, and derived MOFs can be rationally designed to meet the requirements of basic thermal responsiveness, functional integration, and multimodal combination therapy. Through precise modulation of pore dimensions, metal node composition, and ligand structures, these materials can achieve efficient local temperature elevation, targeted delivery to deep-seated tumors, and controlled therapeutic payload release. In PTT, MOFs can efficiently absorb near-infrared light via π-conjugated ligands and metal nodes, converting it into heat through non-radiative relaxation processes, while their porous structures facilitate uniform thermal distribution within the tumor microenvironment. In MWH, the conversion of microwave energy into heat is mediated by ion confinement effects and dielectric or magnetic loss mechanisms, which can additionally induce ROS generation and enable controlled drug release, thereby promoting

synergistic outcomes when combined with CT, PDT, or CDT. Surface functionalization further enhances tumor-targeting efficiency and *in vivo* stability, providing a robust foundation for the potential clinical translation of MOF-based hyperthermia platforms.

Future research should prioritize structural optimization, refinement of multimodal combination strategies, enhancement of deep-tissue targeting, and mitigation of tumor thermal resistance, in parallel with comprehensive evaluation of biocompatibility and biodegradability. By integrating rational material design with precise therapeutic strategies, MOFs have the potential to serve as highly efficient, controllable, and safe platforms for minimally invasive tumor hyperthermia, thereby providing a solid foundation for the development of clinically translatable, precision oncology interventions.

Author Contributions

D.F.: conceptualization, writing—original draft preparation, writing—reviewing and editing; L.G.: writing—review & editing, supervision. Both authors have read and agreed to the published version of the manuscript.

Funding

This research received no external funding.

Institutional Review Board Statement

Not applicable.

Informed Consent Statement

Not applicable.

Data Availability Statement

Not applicable.

Conflicts of Interest

Given the role as the editorial board member, L.G. had no involvement in the peer review of this paper and had no access to information regarding its peer-review process. Full responsibility for the editorial process of this paper was delegated to another editor of the journal.

Use of AI and AI-Assisted Technologies

During the preparation of this work, the authors used ChatGPT to polish language. After using this tool, the authors reviewed and edited the content as needed and take full responsibility for the content of the published article.

References

1. Charbonneau, A.; Brady, A.; Coon, T.; et al. Abstract 1064: Cancer Data Aggregator: A New Cancer Data Discovery Tool. *Cancer Res.* **2025**, *85*, 1064.
2. Bray, F.; Laversanne, M.; Sung, H.; et al. Global Cancer Statistics 2022: GLOBOCAN Estimates of Incidence and Mortality Worldwide for 36 Cancers in 185 Countries. *CA Cancer J. Clin.* **2024**, *74*, 229–263.
3. Mohanty, S.P.; Pai Kanhangad, M.; Kundangar, R. The Extended Posterior Approach for Resection of Sacral Tumours. *Eur. Spine J.* **2019**, *28*, 1461–1467.
4. Wu, Y.; Song, Y.; Wang, R.; et al. Molecular Mechanisms of Tumor Resistance to Radiotherapy. *Mol. Cancer* **2023**, *22*, 96.
5. Akakuru, O.U.; Zhang, Z.; Iqbal, M.Z.; et al. Chemotherapeutic Nanomaterials in Tumor Boundary Delineation: Prospects for Effective Tumor Treatment. *Acta Pharm. Sin. B* **2022**, *12*, 2640–2657.
6. Shirmanova, M.V.; Sinyushkina, S.D.; Komarova, A.D. Metabolic Heterogeneity of Tumors. *Mol. Biol.* **2023**, *57*, 1130–1149.
7. Dang, N.; Waer, M.; Sprangers, B.; et al. Establishment of Operational Tolerance to Sustain Antitumor Immunotherapy. *J. Heart Lung Transplant.* **2022**, *41*, 568–577.
8. Anderson, N.M.; Simon, M.C. The Tumor Microenvironment. *Curr. Biol.* **2020**, *30*, R921–R925.
9. Peter, D.; Ogawa, S.; Elhanani, O.; et al. Tumor Heterogeneity. *Cancer Cell* **2021**, *39*, 1015–1017.
10. Lang, J.A.; Bhalla, S.; Ganeshan, D.; et al. Side Effects of Oncologic Treatment in the Chest: Manifestations at FDG PET/CT. *RadioGraphics* **2021**, *41*, 2071–2089.

11. van den Boogaard, W.M.C.; Komninos, D.S.J.; Vermeij, W.P. Chemotherapy Side-Effects: Not All DNA Damage Is Equal. *Cancers* **2022**, *14*, 627–642.
12. Lugat, A.; Drui, D.; Baron, S.; et al. Effets Secondaires Endocriniens de la Radiothérapie: Diagnostic, Prévention et Traitements. *Cancer/Radiothérapie* **2022**, *26*, 1078–1089.
13. Diez de los Rios de la Serna, C.; Boers-Doets, C.B.; Wiseman, T.; et al. Early Recognition and Management of Side Effects Related to Systemic Anticancer Therapy for Advanced Breast Cancer. *Semin. Oncol. Nurs.* **2024**, *40*, 151553.
14. Xie, G.; Li, B.; Guo, S.; et al. Nonmetallic Magnetic Hyperthermia and Chemo-Immunotherapy of Tumors. *Mater. Today Bio* **2025**, *32*, 101910.
15. Markezana, A.; Goldberg, S.N.; Kumar, G.; et al. Incomplete Thermal Ablation of Tumors Promotes Increased Tumorigenesis. *Int. J. Hyperthermia* **2021**, *38*, 263–272.
16. Lyon, P.C.; Suomi, V.; Jakeman, P.; et al. Quantifying Cell Death Induced by Doxorubicin, Hyperthermia or HIFU Ablation with Flow Cytometry. *Sci. Rep.* **2021**, *11*, 4404.
17. Kirui, D.K.; Koay, E.J.; Guo, X.; et al. Tumor Vascular Permeabilization Using Localized Mild Hyperthermia to Improve Macromolecule Transport. *Nanomedicine* **2014**, *10*, 1487–1496.
18. Huang, Y.; Wei, D.; Wang, B.; et al. NIR-II Light Evokes DNA Cross-Linking for Chemotherapy and Immunogenic Cell Death. *Acta Biomater.* **2023**, *160*, 198–210.
19. Ahmed, K.; Zaidi, S.F.; Rehman, M.-U.; et al. Hyperthermia and Protein Homeostasis: Cytoprotection and Cell Death. *J. Therm. Biol.* **2020**, *91*, 102615.
20. Wang, M.; Chen, Q.; Xu, D.; et al. Self-Cycling Redox Nanoplatform in Synergy with Mild Magnetothermal and Autophagy Inhibition for Efficient Cancer Therapy. *Nano Today* **2022**, *43*, 101374.
21. Yan, Z.; Wu, X.; Tan, W.; et al. Single-Atom Cu Nanozyme-Loaded Bone Scaffolds for Ferroptosis-Synergized Mild Photothermal Therapy in Osteosarcoma Treatment. *Adv. Healthcare Mater.* **2024**, *13*, e2304595.
22. Xiao, L.; Wang, Q.; Hu, J.; et al. pH-Responsive Biodegradable Nanozymes for Mild NIR-II Hyperthermia-Enhanced Tumor-Specific Chemotherapy and Chemodynamic Therapy. *Appl. Mater. Today* **2024**, *39*, 102280.
23. Deng, Z.; Jiang, C.; Younis, M.R.; et al. Mild Hyperthermia-Enhanced Chemo-Photothermal Synergistic Therapy Using Doxorubicin-Loaded Gold Nanovesicles. *Chin. Chem. Lett.* **2021**, *32*, 2411–2414.
24. Ma, K.; Wang, L.; Li, W.; et al. Turning Cold into Hot: Emerging Strategies to Fire Up the Tumor Microenvironment. *Trends Cancer* **2025**, *11*, 117–134.
25. Kong, X.-X.; Jiang, S.; Liu, T.; et al. Paclitaxel Increases Sensitivity of SKOV3 Cells to Hyperthermia by Inhibiting Heat Shock Protein 27. *Biomed. Pharmacother.* **2020**, *132*, 110907.
26. Kim, C.; Guo, Y.; Velalopoulou, A.; et al. Closed-Loop Trans-Skull Ultrasound Hyperthermia Leads to Improved Drug Delivery from Thermosensitive Drugs and Promotes Changes in Vascular Transport Dynamics in Brain Tumors. *Theranostics* **2021**, *11*, 7276–7293.
27. Li, B.; Fu, G.; Liu, C.; et al. Ti_2C_3 MXene-Based Nanocomposite as an Intelligent Nanoplatform for Efficient Mild Hyperthermia Treatment. *J. Colloid Interface Sci.* **2024**, *665*, 389–398.
28. Marchant, E.D.; Kaluhiokalani, J.P.; Wallace, T.E.; et al. Localized Heat Therapy Improves Mitochondrial Respiratory Capacity but Not Fatty Acid Oxidation. *Int. J. Mol. Sci.* **2022**, *23*, 8500.
29. Covarrubias, G.; Lorkowski, M.E.; Sims, H.M.; et al. Hyperthermia-Mediated Changes in the Tumor Immune Microenvironment Using Iron Oxide Nanoparticles. *Nanoscale Adv.* **2021**, *3*, 5890–5899.
30. Carter, T.J.; Agliardi, G.; Lin, F.-Y.; et al. Potential of Magnetic Hyperthermia to Stimulate Localized Immune Activation. *Small* **2021**, *17*, e2005241.
31. Lee, T.H.; Bu, J.; Kim, B.H.; et al. Sub-Lethal Hyperthermia Promotes Epithelial-to-Mesenchymal-Like Transition of Breast Cancer Cells: Implication of the Synergy between Hyperthermia and Chemotherapy. *RSC Adv.* **2019**, *9*, 52–57.
32. Zhang, Y.; Gao, X.; Yan, B.; et al. Enhancement of $CD8^+$ T-Cell-Mediated Tumor Immunotherapy via Magnetic Hyperthermia. *ChemMedChem* **2022**, *17*, e202100656.
33. Wang, Y.; Hong, W.; Che, S.; et al. Outcomes for Hyperthermia Combined with Concurrent Radiochemotherapy for Patients with Cervical Cancer. *Int. J. Radiat. Oncol. Biol. Phys.* **2020**, *107*, 499–511.
34. Lassche, G.; Crezee, J.; Van Herpen, C.M.L. Whole-Body Hyperthermia in Combination with Systemic Therapy in Advanced Solid Malignancies. *Crit. Rev. Oncol. Hematol.* **2019**, *139*, 67–74.
35. Li, Y.; Ma, X.; Liu, X.; et al. Redox-Responsive Functional Iron Oxide Nanocrystals for Magnetic Resonance Imaging-Guided Tumor Hyperthermia Therapy and Heat-Mediated Immune Activation. *ACS Appl. Nano Mater.* **2022**, *5*, 4537–4549.
36. Chiang, C.-F.; Hsu, Y.-H.; Liu, C.-C.; et al. Pulsed-Wave Ultrasound Hyperthermia Enhanced Nanodrug Delivery Combined with Chloroquine Exerts Effective Antitumor Response and Postpones Recurrence. *Sci. Rep.* **2019**, *9*, 12448.
37. Singh, G.; Paul, A.; Shekhar, H.; et al. Pulsed Ultrasound Assisted Thermo-Therapy for Subsurface Tumor Ablation: A Numerical Investigation. *J. Therm. Sci. Eng. Appl.* **2021**, *13*, 041010.

38. Mohanty, B.; Kumari, S.; Yadav, P.; et al. Metal-Organic Frameworks (MOFs) and MOF Composites Based Biosensors. *Coord. Chem. Rev.* **2024**, *519*, 216102.
39. Qi, X.; Chen, Q.; Chang, Z.; et al. Breaking Pore Size Limit of Metal-Organic Frameworks: Bio-Etched ZIF-8 for Lactase Immobilization and Delivery *in Vivo*. *Nano Res.* **2022**, *15*, 5646–5652.
40. Bisercic, M.S.; Marjanovic, B.; Zasonska, B.A.; et al. Novel Microporous Composites of MOF-5 and Polyaniline with High Specific Surface Area. *Synth. Met.* **2020**, *262*, 116348.
41. Deng, X.; Li, J.; Zhao, B.; et al. Design of a Novel Ag-MOF@GO Composite with a High Specific Surface Area and Structural Stability for the Efficient Removal of Malachite Green. *New J. Chem.* **2023**, *47*, 16022–16029.
42. Wu, J.; Jiang, S.; Xie, W.; et al. Surface Modification of the Ti Surface with Nanoscale Bio-MOF-1 for Improving Biocompatibility and Osteointegration in Vitro and *in Vivo*. *J. Mater. Chem. B* **2022**, *10*, 8535–8548.
43. Bachinin, S.; Marunchenko, A.; Zhestkij, N.; et al. Metal-Organic Framework Single Crystal Infrared Photodetector. *Photonics Nanostruct. Fundam. Appl.* **2023**, *55*, 101145.
44. Li, J.; Yan, Y.; Chen, Y.; et al. Flexible Curcumin-Loaded Zn-MOF Hydrogel for Long-Term Drug Release and Antibacterial Activities. *Int. J. Mol. Sci.* **2023**, *24*, 11439.
45. Wang, Y.; Xu, S.; Shi, L.; et al. Cancer-Cell-Activated in Situ Synthesis of Mitochondria-Targeting AIE Photosensitizer for Precise Photodynamic Therapy. *Angew. Chem. Int. Ed.* **2021**, *60*, 14945–14953.
46. Ma, X.; Pan, F.; Xiu, Z.; et al. Bridging Dielectric-Magnetic Synergistic Units with MOFs on Fibers Structure for High-Efficient Microwave Absorption at Low Filler Loading. *Carbon* **2024**, *229*, 119444.
47. Lin, J.-Y.; Wang, H.; Oh, W.D.; et al. Integrated MOF-Mesh and TEMPO-Grafted Carbon Fiber as a Sandwich-Like Catalytic System for Selective Valorization of Lignin-Derived Compound under Microwave Irradiation. *Chem. Eng. J.* **2021**, *411*, 128605.
48. Hong, D.; Zhang, K.; Yang, M.; et al. Effects of MOF-MoO_{3-x} Derivatives Synthesis and Oxygen Defect Engineering on Photocatalytic CO_2 Reduction. *Ceram. Int.* **2024**, *50*, 47042–47050.
49. Abbas, M.; Bisht, S.; Murari, B.; et al. Structural and Magnetic Study of Fluorinated Gadolinium Metal-Organic Frameworks. *Cryst. Growth Des.* **2025**, *25*, 5183–5192.
50. Wang, D.; Zhou, J.; Shi, R.; et al. Biodegradable Core-Shell Dual-Metal-Organic-Frameworks Nanotheranostic Agent for Multiple Imaging Guided Combination Cancer Therapy. *Theranostics* **2017**, *7*, 4605–4617.
51. Nikazar, S.; Barani, M.; Rahdar, A.; et al. Photo- and Magnetothermally Responsive Nanomaterials for Therapy, Controlled Drug Delivery and Imaging Applications. *ChemistrySelect* **2020**, *5*, 12590–12609.
52. Pillai, N.G.; Knavaneeth, A.; Rhee, K.Y.; et al. PEGylation of a Shell over Core-Shell MOFs—A Novel Strategy for Preventing Agglomeration and Synergism in Terms of Physicochemical and Biological Properties. *J. Mater. Chem. B* **2023**, *11*, 10665–10677.
53. Hintz, H.; Wuttke, S. Postsynthetic Modification of an Amino-Tagged MOF Using Peptide Coupling Reagents: A Comparative Study. *Chem. Commun.* **2014**, *50*, 11472–11475.
54. Falsafi, M.; Zahiri, M.; Saljooghi, A.S.; et al. Aptamer Targeted Red Blood Cell Membrane-Coated Porphyrinic Copper-Based MOF for Guided Photochemotherapy against Metastatic Breast Cancer. *Microporous Mesoporous Mater.* **2021**, *325*, 111337.
55. Liu, J.; Yang, L.; Cao, X.; et al. PEGylated Mn Containing MOF Nanoparticles for Potential Immunotherapy of Pancreatic Cancer via Manganese Induced Activation of Anti-Tumor Immunity. *Colloid Interface Sci. Commun.* **2021**, *42*, 100409.
56. Jiang, H.; Xia, W.; Xia, T.; et al. Chemotactic Recruitment of Genetically Engineered Cell Membrane-Camouflaged Metal-Organic Framework Nanoparticles for Ischemic Osteonecrosis Treatment. *Acta Biomater.* **2024**, *185*, 410–428.
57. Liu, W.; Li, Y.; Wang, Y.; et al. Bioactive Metal-Organic Frameworks as a Distinctive Platform to Diagnosis and Treat Vascular Diseases. *Small* **2024**, *20*, 2310249.
58. Oh, J.Y.; Jana, B.; Seong, J.; et al. Unveiling the Power of Cloaking Metal-Organic Framework Platforms via Supramolecular Antibody Conjugation. *ACS Nano* **2024**, *18*, 15790–15801.
59. Nangare, S.; Ramraje, G.; Patil, P. Formulation of Lactoferrin Decorated Dextran Based Chitosan-Coated Europium Metal-Organic Framework for Targeted Delivery of Curcumin. *Int. J. Biol. Macromol.* **2024**, *259*, 129325.
60. Tabish, T.A.; Hussain, M.Z.; Fischer, R.A.; et al. Mitochondria-Targeted Metal-Organic Frameworks for Cancer Treatment. *Mater. Today* **2023**, *66*, 302–320.
61. Chen, J.; Li, Y. The Road to MOF-Related Functional Materials and Beyond: Desire, Design, Decoration, and Development. *Chem. Rec.* **2016**, *16*, 1456–1476.
62. Benecke, J.; Mangelsen, S.; Engesser, T.A.; et al. A Porous and Redox Active Ferrocenedicarboxylic Acid Based Aluminium MOF with a MIL-53 Architecture. *Dalton Trans.* **2019**, *48*, 16737–16743.
63. Kouser, S.; Hezam, A.; Khanum, S.A. Synthesis, Characterization, and Catalytic Activity of Zinc-Isonicotinic Acid MOF. *J. Mol. Struct.* **2025**, *1321*, 140061.
64. Mínguez Espallargas, G.; Coronado, E. Magnetic Functionalities in MOFs: From the Framework to the Pore. *Chem. Soc. Rev.* **2018**, *47*, 533–557.

65. Li, T.; Wu, Q.; Wang, W.; et al. MOF-Derived Nano-Popcorns Synthesized by Sonochemistry as Efficient Sensitizers for Tumor Microwave Thermal Therapy. *Biomaterials* **2020**, *234*, 119773.
66. Hao, Q.; Han, T.; Yang, Y.; et al. Multifunctional Dual-Ligand MOF for Capture, Imaging, and Photodynamic Clearance of Circulating Tumor Cells. *Anal. Chem.* **2025**, *97*, 23269–23279.
67. Nguyen, M.V.; Dong, H.C.; Truong, V.T.N.; et al. A New Porphyrinic Vanadium-Based MOF Constructed from Infinite $V(OH)O_4$ Chains: Syntheses, Characterization and Photoabsorption Properties. *New J. Chem.* **2022**, *46*, 632–641.
68. Jiang, M.; Weng, Y.-G.; Zhou, Z.-Y.; et al. Cobalt Metal-Organic Frameworks Incorporating Redox-Active Tetrathiafulvalene Ligand: Structures and Effect of LLCT within the MOF on Photoelectrochemical Properties. *Inorg. Chem.* **2020**, *59*, 10727–10735.
69. Rabiee, N. Sustainable Metal-Organic Frameworks (MOFs) for Drug Delivery Systems. *Mater. Today Commun.* **2023**, *35*, 106244.
70. Schlachter, A.; Asselin, P.; Harvey, P.D. Porphyrin-Containing MOFs and COFs as Heterogeneous Photosensitizers for Singlet Oxygen-Based Antimicrobial Nanodevices. *ACS Appl. Mater. Interfaces* **2021**, *13*, 26651–26672.
71. Liu, S.; Xin, R.; Zhang, X.; et al. Separable Microneedle Patch Integrated with the Dictamnine-Loaded Copper MOF Nanozyme for Atopic Dermatitis Treatment. *ACS Appl. Mater. Interfaces* **2025**, *17*, 26386–26401.
72. Zhang, B.; Chen, J.; Zhu, Z.; et al. Advances in Immunomodulatory MOFs for Biomedical Applications. *Small* **2024**, *20*, e2307299.
73. Díaz, J.C.; Glatz, J.; Olivas, E.M.; et al. Direct Synthesis of High-Valence Protein@UiO-66 Composites: Linking Crystallization Pathways to Protein Encapsulation. *Adv. Mater.* **2026**, *38*, e21603.
74. Wang, D.; Wu, H.; Zhou, J.; et al. *In Situ* One-Pot Synthesis of MOF-Polydopamine Hybrid Nanogels with Enhanced Photothermal Effect for Targeted Cancer Therapy. *Adv. Sci.* **2018**, *5*, 1800287.
75. Tajahmadi, S.; Bagri, F.; Shojaei, A.; et al. A Novel Dual-Functional Quercetin Carrier Based on Gd-MOF for Drug Delivery and MR Imaging. *Mater. Des.* **2026**, *262*, 115570.
76. Zhao, C.; Xu, Y.; Xiao, F.; et al. Perfluorooctane Sulfonate Removal by Metal-Organic Frameworks (MOFs): Insights into the Effect and Mechanism of Metal Nodes and Organic Ligands. *Chem. Eng. J.* **2021**, *406*, 126852.
77. Zhang, N.; Feng, X.; Rao, D.; et al. Lattice Oxygen Activation Enabled by High-Valence Metal Sites for Enhanced Water Oxidation. *Nat. Commun.* **2020**, *11*, 4066.
78. Takhsha, M.; Cabassi, R.; Cavazzini, G.; et al. Self-Regulating Magnetic Hyperthermia by Magnetostructural Phase Transformation of Magnetic-Shape-Memory Ni–Mn–Cu-Ga Heusler-Type Particles. *Mater. Today Chem.* **2025**, *48*, 103006.
79. Zhang, S.; Liu, G.; Lv, S.; et al. Ti-MOF@Metal-Polyphenol Network Derived $TiN_{0.9}$@NC/Magnetic MWCNTs Composites for Microwave Absorption. *Chem. Eng. J.* **2023**, *468*, 143763.
80. Subramaniyam, V.; Ravi, P.V.; Pichumani, M. Structure Co-ordination of Solitary Amino Acids as Ligands in Metal-Organic Frameworks (MOFs): A Comprehensive Review. *J. Mol. Struct.* **2022**, *1251*, 131931.
81. Ranjbar, K.; Masoudpanah, S.M.; Koohdar, H.R. MOF-Derived $NiCo_2O_4$/NiO Nanocomposites as Microwave Absorbers: Effects of Organic Ligands. *J. Mol. Liq.* **2024**, *394*, 123779.
82. Wang, H.; Gu, M.; Huang, X.; et al. Ligand-Based Modulation of the Electronic Structure at Metal Nodes in MOFs to Promote the Oxygen Evolution Reaction. *J. Mater. Chem. A* **2023**, *11*, 7239–7245.
83. Qin, L.; Zhao, Y.-X.; Liu, Q.; et al. Tuning the Organic Ligands to Optimize the Nitrogen Reduction Performance of Co(II) or Ni(II)-Based MOFs. *Mater. Chem. Front.* **2024**, *8*, 3203–3213.
84. Panda, S.; Kundu, S.; Malik, P.; et al. Leveraging Metal Node-Linker Self-Assembly to Access Functional Anisotropy of Zirconium-Based MOF-on-MOF Epitaxial Heterostructure Thin Films. *Chem. Sci.* **2024**, *15*, 2586–2592.
85. Qin, L.; Zheng, Q.-M.; Liu, J.-L.; et al. A Novel and Efficient Method of MOF-Derived Electrocatalyst for HER Performance through Doping Organic Ligands. *Mater. Chem. Front.* **2021**, *5*, 7833–7842.
86. Li, X.; Wang, R.; Zhao, H.; et al. Co-MOFs with 1,1′-(5-Methyl-1,3-phenylene)bis(1H-imidazole) and Aromatic Carboxylates as Coligands: Synthesis, Structure, and Spectroscopic and Thermal Characterizations. *J. Coord. Chem.* **2016**, *69*, 2247–2262.
87. Xian, J.-Y.; Xie, X.-X.; Huang, Z.-Y.; et al. Structure and Properties of a Mixed-Ligand Co-MOF That Was Synthesized in Situ from a Single Imidazole-Pyridyl-Tetrazole Trifunctional Ligand. *Cryst. Growth Des.* **2023**, *23*, 1448–1454.
88. Ha, J.; Moon, H.R. Synthesis of MOF-on-MOF Architectures in the Context of Interfacial Lattice Matching. *CrystEngComm* **2021**, *23*, 2337–2354.
89. Dong, M.; Zhou, H.; Cao, Q.; et al. Rational Design and Controlled Synthesis of MOF-on-MOF Heterostructures: Overcoming Lattice Mismatch. *Chem. Eng. Sci.* **2026**, *327*, 123651.
90. Chang, L.-M.; Ma, Z.-Z.; Huang, J.; et al. Liquid-Phase Epitaxial Growth of Multiple MOF Thin Films with High Lattice Mismatch. *Inorg. Chem. Front.* **2023**, *10*, 1136–1142.
91. Jian, C.; Xuejiao, L.; Hongqi, T. Metal-Organic Framework (MOF)-Based Drug Delivery. *Curr. Med. Chem.* **2020**, *27*, 5949–5969.

92. Tomalia, N.A.; Rakova, Y.; Tubman, A.N.; et al. Tunable on-Demand Explosives Derived from Isoreticular Metal-Organic Framework Nanocomposites. *Chem. Mater.* **2026**, *38*, 2055–2062.
93. Boopalan, A.S.; Rahulan, K.M.; Little Flower, N.A.; et al. Synergistic Effects of Europium Doping on MOF-5: Exploring Its Photoluminescent and Non-Linear Optical Behaviour for Enhanced Optical Limiting. *Nanoscale* **2025**, *17*, 8836–8849.
94. Zhao, W.; Guo, Z.; Lan, D.; et al. Construction of Multicomponent Bimetallic MOF-Derived Transition Metal Sulfide Composites for Electromagnetic Wave Absorption. *Small* **2025**, *21*, e2409339.
95. Guo, Y.; Zhu, Y.; Sun, J.; et al. MOF-Derived Carbon Nanotube Bridged Co/MoC@NC Composites for Enhanced Electromagnetic Wave Absorption. *J. Alloys Compd.* **2025**, *1010*, 177346.
96. Wang, Y.; Ban, Y.; Hu, Z.; et al. Hetero-Lattice Intergrown and Robust MOF Membranes for Polyol Upgrading. *Angew. Chem. Int. Ed.* **2022**, *61*, e202114479.
97. Wang, J.; Qin, J.; Zhu, H.; et al. MOF-Based Hierarchically Porous Monoliths Prepared via High Internal Phase Emulsion Template: Morphology, Thermal Stability, Mechanical Property, and MOF Accessibility. *Macromol. Mater. Eng.* **2022**, *307*, 2200309.
98. Yang, L.; Xu, T.; Zou, H.; et al. Self-Assembled Fluorescent Zn-MOF with High Specific Surface Area Based on the Coordination Interaction for Sensitive Detection and Selective Removal of Tetracycline Antibiotic in Water. *Opt. Mater.* **2024**, *157*, 116126.
99. Wang, S.-M.; Mu, X.-T.; Liu, H.-R.; et al. Pore-Structure Control in Metal-Organic Frameworks (MOFs) for Capture of the Greenhouse Gas SF_6 with Record Separation. *Angew. Chem. Int. Ed.* **2022**, *61*, e202207066.
100. Indra, A.; Song, T.; Paik, U. Metal Organic Framework Derived Materials: Progress and Prospects for the Energy Conversion and Storage. *Adv. Mater.* **2018**, *30*, 1705146.
101. Zheng, X.; Chen, L.; Zhang, H.; et al. Optimized Sieving Effect for Ethanol/Water Separation by Ultramicroporous MOFs. *Angew. Chem. Int. Ed.* **2023**, *62*, e202216710.
102. Hu, A.; Xie, Q.; Chen, L.; et al. Hierarchically Ordered Meso-/Macroporous MOF-Based Materials for Catalysis and Energy Applications. *EnergyChem* **2024**, *6*, 100137.
103. Li, T.; Kozlowski, M.T.; Doud, E.A.; et al. Stepwise Ligand Exchange for the Preparation of a Family of Mesoporous MOFs. *J. Am. Chem. Soc.* **2013**, *135*, 11688–11691.
104. Ambroz, F.; Macdonald, T.J.; Martis, V.; et al. Evaluation of the BET Theory for the Characterization of Meso and Microporous MOFs. *Small Methods* **2018**, *2*, 1800173.
105. Laybourn, A.; Katrib, J.; Ferrari-John, R.S.; et al. Metal–Organic Frameworks in Seconds via Selective Microwave Heating. *J. Mater. Chem. A* **2017**, *5*, 7333–7338.
106. Sun, M.; Li, Z.; Wei, B.; et al. MOFs Derived Fe/Co/C Heterogeneous Composite Absorbers for Efficient Microwave Absorption. *Synth. Met.* **2023**, *292*, 117229.
107. Ma, X.; Cai, C.; Sun, W.; et al. Enhancing Energetic Performance of Multinuclear Ag(I)-Cluster MOF-Based High-Energy-Density Materials by Thermal Dehydration. *ACS Appl. Mater. Interfaces* **2019**, *11*, 9233–9238.
108. Cao, Y.; Abazari, R.; Li, Q.; et al. Dynamic Interfaces in Metal–Organic Frameworks. *Chem. Soc. Rev.* **2026**, *55*, 5227–5268.
109. Mallik, S.; Chand Pal, S.; Mondal, S.; et al. Stress-Driven Recrystallization of Pentacene Films via Diffusion-Induced Ingress of MOF Nanocrystals into the Grain Boundaries. *Appl. Surf. Sci.* **2024**, *654*, 159420.
110. Zhu, Y.; Zhang, Z.; Li, W.; et al. Highly Exposed Active Sites of Defect-Enriched Derived MOFs for Enhanced Oxygen Reduction Reaction. *ACS Sustain. Chem. Eng.* **2019**, *7*, 17855–17862.
111. Sun, C.; Lan, D.; Jia, Z.; et al. Kirkendall Effect-Induced Ternary Heterointerfaces Engineering for High Polarization Loss MOF-LDH-MXene Absorbers. *Small* **2024**, *20*, e2405874.
112. Schlachter, A.; Asselin, P.; Fortin, D.; et al. Strong Host–Guest Dependence on the Emissive Properties of MOF-5 and $[Zn_2(BTTB)(DMF)_2 \cdot (H_2O)_3]_n$. *Inorg. Chem.* **2023**, *62*, 13757–13764.
113. Chen, Y.; Wang, P.; Yu, F.; et al. Ciprofloxacin Self-Promoted Degradation Mechanism: Local Symmetry-Breaking of MOF Driven Radical-Dipole Cooperativity for Enhanced Charge Carrier Separation. *Chem. Eng. J.* **2025**, *527*, 171607.
114. Qu, L.; Xu, Y.; Cui, W.; et al. Trends in Conductive MOFs for Sensing: A Review. *Anal. Chim. Acta* **2025**, *1336*, 343307.
115. Ning, Y.; Jiang, X.; Huang, J.; et al. Trimetallic MOFs Derived $NiFe_2O_4$/$MoNi_4$-NC Schottky Heterojunctions with Abundant Defects and Dielectric-Magnetic Coupling for Electromagnetic Response. *J. Mater. Sci. Technol.* **2025**, *213*, 1–13.
116. Babal, A.S.; Chaudhari, A.K.; Yeung, H.H.M.; et al. Guest-Tunable Dielectric Sensing Using a Single Crystal of HKUST-1. *Adv. Mater. Interfaces* **2020**, *7*, 2000408.
117. Lee, G.; Lee, S.; Oh, S.; et al. Tip-To-Middle Anisotropic MOF-on-MOF Growth with a Structural Adjustment. *J. Am. Chem. Soc.* **2020**, *142*, 3042–3049.
118. Han, G.-Y.; Sun, M.; Zhao, R.; et al. Defect Engineered Ti-MOFs and Their Applications. *Chem. Soc. Rev.* **2025**, *54*, 5081–5107.
119. Shan, Y.; Zhang, G.; Shi, Y.; et al. Synthesis and Catalytic Application of Defective MOF Materials. *Cell Rep. Phys. Sci.* **2023**, *4*, 101301.

120. Li, N.; Li, H.; Ji, R.; et al. Fabrication of Bimetallic MOF with 2D Nanosheets Structure and Rich Active Sites for Enhanced Removal of Organic Pollutants by Activation of Peroxymonosulfate. *J. Environ. Chem. Eng.* **2023**, *11*, 110607.
121. Shen, X.; Ma, Y.; Luo, H.; et al. Peptide Aptamer-Paclitaxel Conjugates for Tumor Targeted Therapy. *Molecules* **2025**, *30*, 40.
122. Zhang, R.; Hu, Q.; Yang, S.; et al. MOF-Fe@C Nanocomposites for Microwave Absorption. *Adv. Eng. Mater.* **2024**, *26*, 2400527.
123. Li, K.; Liu, Y.; Yan, Y.; et al. Cross-Scale Regulation of MOF-Derived Gradient Heterointerfaces for Microwave Absorption. *Adv. Funct. Mater.* **2026**, *36*, e75348.
124. Zorlu, T.; Hetey, D.; Reithofer, M.R.; et al. Physicochemical Methods for the Structuring and Assembly of MOF Crystals. *Acc. Chem. Res.* **2024**, *57*, 2105–2116.
125. Li, L.; Meng, C.; Xu, C.; et al. Morphology-Engineered MOFs for Advanced Carbon Capture and Separation: From Zero-Dimensional Particles to Three-Dimensional Architectures. *Renew. Sustain. Energy Rev.* **2026**, *237*, 117018.
126. Zhou, C.; Pan, M.; Li, S.; et al. Metal Organic Frameworks (MOFs) as Multifunctional Nanoplatform for Anticorrosion Surfaces and Coatings. *Adv. Colloid Interface Sci.* **2022**, *305*, 102707.
127. Liu, J.; Cao, Q.; Meng, C.; et al. Composition Manipulation of Heat-Resistant Iron-Based Cores@Graphitic Carbon@Amorphous Carbon Derived from Urea-Modulated MOFs for High-Efficient Microwave Absorption. *Ceram. Int.* **2022**, *48*, 23348–23356.
128. Zhang, G.; Chang, L.; Xu, X.; et al. Ultrasmall Iridium-Encapsulated Porphyrin Metal-Organic Frameworks for Enhanced Photodynamic/Catalytic Therapy by Producing Reactive Oxygen Species Storm. *J. Colloid Interface Sci.* **2025**, *677*, 1022–1033.
129. Xie, Z.; Zhao, H.; Chen, F.; et al. Magnetically Aligned Co-C/MWCNT/Polyacrylamide with Directional Thermal Conduction for Enhanced Electromagnetic Wave Absorption by Synergistic Engineering of Dielectric and Magnetic Loss. *Diam. Relat. Mater.* **2025**, *157*, 112519.
130. Luo, X.; Sun, H.-Y.; Lu, S.-Y.; et al. Fe-Doped Cu-Based Bimetallic Metal–Organic Frameworks as Nanoscale Microwave Sensitizers for Enhancing Microwave Thermal and Dynamic Therapy for Hepatocellular Carcinoma. *Nanoscale* **2024**, *16*, 11069–11080.
131. Wang, J.; Deng, S.-Q.; Zhao, T.-T.; et al. A Mn(II)-MOF with Inherent Missing Metal-Ion Defects Based on an Imidazole-Tetrazole Tripodal Ligand and Its Application in Supercapacitors. *Dalton Trans.* **2020**, *49*, 12150–12155.
132. Yao, X.; He, Y.; Fu, S.; et al. Bimetallic MOF-Derived CeO_2/Co_3O_4 Microflowers with Synergy of Oxygen Vacancy and p-n Heterojunction for High-Performance n-Butanol Sensors. *Mater. Today Commun.* **2022**, *33*, 104445.
133. Chen, J.; Hang, X.; Du, M.; et al. Intermolecular Forces-Oriented Growth of MOF-on-MOF Heterostructures. *Chem. Eur. J.* **2025**, *31*, e202403746.
134. Ren, J.; Ledwaba, M.; Musyoka, N.M.; et al. Structural Defects in Metal-Organic Frameworks (MOFs): Formation, Detection and Control towards Practices of Interests. *Coord. Chem. Rev.* **2017**, *349*, 169–197.
135. El-Boubbou, K.; Lemine, O.M.; Algessair, S.; et al. Preparation and Characterization of Various PVPylated Divalent Metal-Doped Ferrite Nanoparticles for Magnetic Hyperthermia. *RSC Adv.* **2024**, *14*, 15664–15679.
136. Chen, L.; Zhao, D.; Ren, X.; et al. Shikonin-Loaded Hollow Fe-MOF Nanoparticles for Enhanced Microwave Thermal Therapy. *ACS Biomater. Sci. Eng.* **2023**, *9*, 5405–5417.
137. Cai, X.; Zhao, Y.; Wang, L.; et al. Synthesis of Au@MOF Core-Shell Hybrids for Enhanced Photodynamic/Photothermal Therapy. *J. Mater. Chem. B* **2021**, *9*, 6646–6657.
138. Dong, J.; Boukhvalov, D.W.; Lv, C.; et al. Enhancing the Electrocatalytic Activity of Metal–Organic Frameworks in the Oxygen Evolution Reaction by Introducing High-Valent Metal Centers. *J. Mater. Chem. A* **2023**, *11*, 16683–16694.
139. Deng, Z.; Fang, C.; Ma, X.; et al. One Stone Two Birds: Zr-Fc Metal-Organic Framework Nanosheet for Synergistic Photothermal and Chemodynamic Cancer Therapy. *ACS Appl. Mater. Interfaces* **2020**, *12*, 20321–20330.
140. Cao, K.; Ye, W.; Zhang, Y.; et al. Fabrication of MOF-rGO Aerogels to Enhance Electromagnetic Wave Absorption by Adjusting the Morphology and Structure of MOFs by Electron Transfer. *Chem. Eng. J.* **2024**, *489*, 151384.
141. Feng, Y.; Chen, Q.; Jin, C.; et al. Microwave-Activated Cu-Doped Zirconium Metal-Organic Framework for a Highly Effective Combination of Microwave Dynamic and Thermal Therapy. *J. Controlled Release* **2023**, *361*, 102–114.
142. Li, H.; Xiao, Z.; Hao, R.; et al. Encapsulating Carbon Quantum Dots by Zr-MOF-Supported Pt Nanoparticles for Enhanced Photothermal RWGS Reaction. *Sep. Purif. Technol.* **2025**, *365*, 132637.
143. He, J.; Zhang, H.; Zhu, J.; et al. Layer-by-Layer Synthesis of Au Nanorods@Metal-Organic Framework Core-Shell Nanohybrids for Magnetic Resonance Imaging Guided Photothermal Therapy. *Mater. Today Commun.* **2022**, *33*, 104560.
144. Kumar, D.; Veena, P.; Singhal, N.; et al. Microneedle-Assisted Transdermal Delivery of Photothermally Active Porous Cu-ZIF-8 MOF Formulations for Localized Combinational Therapy of Cancer. *Surfaces Interfaces* **2026**, *83*, 108566.
145. Wang, J.; Lin, Y.; Wang, T.; et al. Polydopamine-Coated Fe-MOF-NH_2@Pt@PDA Nanoparticles for Multimodal Synergistic Chemodynamic/Sonodynamic/Photothermal Cancer Therapy. *J. Appl. Polym. Sci.* **2025**, *142*, e57542.

146. Jiang, W.; Zhang, H.; Wu, J.; et al. CuS@MOF-Based Well-Designed Quercetin Delivery System for Chemo-Photothermal Therapy. *ACS Appl. Mater. Interfaces* **2018**, *10*, 34513–34523.
147. Ma, R.; Liu, S.; Liu, G.; et al. A Triple-Mode Strategy Combining Low-Temperature Photothermal, Photodynamic, and Chemodynamic Therapies for Treating Infectious Skin Wounds. *Biomater. Sci.* **2024**, *12*, 5521–5533.
148. Khan, I.S.; Garzon-Tovar, L.; Mateo, D.; et al. Metal-Organic-Frameworks and Their Derived Materials in Photo-Thermal Catalysis. *Eur. J. Inorg. Chem.* **2022**, *2022*, e202200316.
149. Jiang, X.; Huang, Z.; Liu, Z.; et al. MOF-Derived Oxygen-Deficient Titania-Mediated Photodynamic/Photothermal-Enhanced Immunotherapy for Tumor Treatment. *ACS Appl. Mater. Interfaces* **2024**, *16*, 34591–34606.
150. Yue, J.; Li, C.; Tao, Y.; et al. Synergistic Defect and Heterojunction Engineering of Carbonized MOF@MoS_2 for Self-Powered Sensing Micro-System with Photothermal Therapy. *Chem. Eng. J.* **2024**, *495*, 153367.
151. Marpaung, F.; Kim, M.; Khan, J.H.; et al. Metal-Organic Framework (MOF)-Derived Nanoporous Carbon Materials. *Chem. Asian J.* **2019**, *14*, 1331–1343.
152. Wang, J.; Zhang, Y.; Ma, Y.; et al. Electrocatalytic Reduction of Carbon Dioxide to High-Value Multicarbon Products with Metal-Organic Frameworks and Their Derived Materials. *ACS Mater. Lett.* **2022**, *4*, 2058–2079.
153. Li, T.; Sun, J.; Yin, Y.; et al. Photothermal/Nitric Oxide Synergistic Anti-Tumour Therapy Based on MOF-Derived Carbon Composite Nanoparticles. *Nanoscale* **2022**, *14*, 16193–16207.
154. Rafiq, K.; Sabir, M.; Abid, M.Z.; et al. Unveiling the Scope and Perspectives of MOF-Derived Materials for Cutting-Edge Applications. *Nanoscale* **2024**, *16*, 16791–16837.
155. Geng, P.; Yu, N.; Macharia, D.K.; et al. MOF-Derived CuS@Cu-MOF Nanocomposites for Synergistic Photothermal-Chemodynamic-Chemo Therapy. *Chem. Eng. J.* **2022**, *441*, 135964.
156. Abdelkareem, M.A.; Abbas, Q.; Sayed, E.T.; et al. Recent Advances on Metal-Organic Frameworks (MOFs) and Their Applications in Energy Conversion Devices: Comprehensive Review. *Energy* **2024**, *299*, 131127.
157. Wang, K.-f.; Mu, Y.-p.; Wang, S.; et al. NIR/pH-Responsive Erythrocyte Membrane-Camouflaged Metal-Organic Framework for Photothermal Therapy of Pancreatic Cancer. *Mater. Today Commun.* **2023**, *34*, 105221.
158. Li, X.; Chen, K.; Guo, R.; et al. Ionic Liquids Functionalized MOFs for Adsorption. *Chem. Rev.* **2023**, *123*, 10432–10467.
159. Du, T.; Qin, Z.; Zheng, Y.; et al. The "Framework Exchange"-Strategy-Based MOF Platform for Biodegradable Multimodal Therapy. *Chem* **2019**, *5*, 2942–2954.
160. Wang, Q.; Astruc, D. State of the Art and Prospects in Metal-Organic Framework (MOF)-Based and MOF-Derived Nanocatalysis. *Chem. Rev.* **2020**, *120*, 1438–1511.
161. Esmailzadeh, F.; Taheri-Ledari, R.; Kashtiaray, A.; et al. Sustainable CelloMOF Cargoes for Regenerative Medicine and Drug Delivery Therapies: A Review. *Ind. Crops Prod.* **2024**, *212*, 118293.
162. Hu, Z.; Zhou, X.; Zhang, W.; et al. Photothermal Amplified Multizyme Activity for Synergistic Photothermal-Catalytic Tumor Therapy. *J. Colloid Interface Sci.* **2025**, *679*, 375–383.
163. Wei, C.; Jin, X.; Wu, C.; et al. Carbon Spheres with High Photothermal Conversion Efficiency for Photothermal Therapy of Tumor. *Diam. Relat. Mater.* **2022**, *126*, 109048.
164. Jiang, J.; Hu, J.; Li, M.; et al. NIR-II Fluorescent Thermophoretic Nanomotors for Superficial Tumor Photothermal Therapy. *Adv. Mater.* **2025**, *37*, 2417440.
165. Wang, D.; Zhou, J.; Chen, R.; et al. Controllable Synthesis of Dual-MOFs Nanostructures for pH-Responsive Artemisinin Delivery, Magnetic Resonance and Optical Dual-Model Imaging-Guided Chemo/Photothermal Combinational Cancer Therapy. *Biomaterials* **2016**, *100*, 27–40.
166. Zhang, X.; Liu, C.; Li, J.; et al. Dual Source-Powered Multifunctional Pt/FePc@Mn-MOF Spindle-Like Janus Nanomotors for Active CT Imaging-Guided Synergistic Photothermal/Chemodynamic Therapy. *J. Colloid Interface Sci.* **2024**, *657*, 799–810.
167. Zhang, Y.; Zhang, G.; Wang, G.; et al. The Synergistic Strategies for the Immuno-Oncotherapy with Photothermal Nanoagents. *WIREs Nanomed. Nanobiotechnol.* **2021**, *13*, e1717.
168. Wang, Z.; Yu, W.; Yu, N.; et al. Construction of CuS@Fe-MOF Nanoplatforms for MRI-Guided Synergistic Photothermal-Chemo Therapy of Tumors. *Chem. Eng. J.* **2020**, *400*, 125877.
169. Wei, L.; Zhang, Y.-M.; Yin, X.-L.; et al. Green-Reduced Biodegradable Core–Shell Smart-Responsive MOFs for Photothermal-Enhanced Chemo-Chemodynamic in Tumor Catalysis Therapy. *Mol. Pharmaceutics* **2025**, *22*, 3433–3446.
170. Zhu, Y.; Huang, Y.; Yan, T.-H.; et al. Metal-Organic Framework-Based Nanoheater with Photo-Triggered Cascade Effects for On-Demand Suppression of Cellular Thermoresistance and Synergistic Cancer Therapy. *Adv. Healthcare Mater.* **2022**, *11*, 2200004.
171. Han, Y.-C.; Liu, M.-L.; Sun, L.; et al. A General Strategy for Overcoming the Trade-Off between Ultrasmall Size and High Loading of MOF-Derived Metal Nanoparticles by Millisecond Pyrolysis. *Nano Energy* **2022**, *97*, 107125.

172. Zhang, Y.; Li, Y.; Lu, J.; et al. A MOF-in-MOF Nanoplatform for Photothermal/Chemodynamic Therapy That Enhances Antitumor Immunity through Targeted Suppression of the COX-2/PGE_2 Axis. *J. Nanobiotechnology* **2026**, in press. https://doi.org/10.1186/s12951-026-04330-4.
173. You, S.; Ding, G.; Chi, B.; et al. Construction a Starving Therapy Induced Photothermal Enhanced Cascade Nanoreactor for Imaging Guided Catalytic Synergistic Therapy of Tumor. *Colloids Surf. A Physicochem. Eng. Asp.* **2023**, *674*, 131941.
174. Nazari, M.; Ramezani, M.; Eshghi, H.; et al. Synthesis of RGD-Dextran-Coated Fe-Porphyrin-Based Zr-MOF for CT/MR Imaging and Targeted Chemo-Photothermal Therapy of Melanoma. *Carbohydr. Polym.* **2025**, *360*, 123614.
175. Zhang, F.; Liu, W.; Hao, Z.; et al. Defect-Engineered Iron Single-Site Catalysts with Tailored Atomic Coordination for Enhanced Mild Photothermal Therapy via Triad Modulation of Apoptosis and Ferroptosis. *BMEMat* **2025**, *4*, e70051.
176. Zhang, Q.; Kuang, G.; Wang, H.; et al. Multi-Bioinspired MOF Delivery Systems from Microfluidics for Tumor Multimodal Therapy. *Adv. Sci.* **2023**, *10*, 2303818.
177. Wu, Y.; Guo, Y.; Feng, K.; et al. MOF-Based Hypocrellin Composite Nanomaterials as Advanced Plant-Derived Photosensitizers for Multimodal Therapy. *Chem. Eng. J.* **2025**, *520*, 166071.
178. Li, Y.; Xu, N.; Zhou, J.; et al. Facile Synthesis of a Metal–Organic Framework Nanocarrier for NIR Imaging-Guided Photothermal Therapy. *Biomater. Sci.* **2018**, *6*, 2918–2924.
179. Wang, L.; Xu, Y.; Liu, C.; et al. Copper-Doped MOF-Based Nanocomposite for GSH Depleted Chemo/Photothermal/ Chemodynamic Combination Therapy. *Chem. Eng. J.* **2022**, *438*, 135567.
180. Zeng, Z.; Fu, C.; Sun, X.; et al. Reversing the Immunosuppressive Microenvironment with Reduced Redox Level by Microwave-Chemo-Immunostimulant Ce-Mn MOF for Improved Immunotherapy. *J. Nanobiotechnology* **2022**, *20*, 512.
181. Wu, Q.; Zhao, L.; Tan, L.; et al. Microwave-Responsive AlEu-MOFs Potentiate NLRP3-Mediated Pyroptosis via a "Triple Initiating" Tactic for Breast Cancer Microwave-Immunotherapy. *Small* **2025**, *21*, 2501157.
182. Elkayal, H.A.; Ismail, N.E. Efficient Focusing of Microwave Hyperthermia for Small Deep-Seated Breast Tumors Treatment Using Particle Swarm Optimization. *Comput. Methods Biomech. Biomed. Eng.* **2021**, *24*, 985–994.
183. Jian, S.; Wu, X.; Yu, H.; et al. Enhancing Strategies of MOFs-Derived Materials for Microwave Absorption: Review and Perspective. *Adv. Colloid Interface Sci.* **2025**, *338*, 103412.
184. Qin, Q.; Yang, M.; Shi, Y.; et al. Mn-Doped Ti-Based MOFs for Magnetic Resonance Imaging-Guided Synergistic Microwave Thermal and Microwave Dynamic Therapy of Liver Cancer. *Bioact. Mater.* **2023**, *27*, 72–81.
185. Yu, H.; Yao, J.; Lv, J.; et al. Low-Temperature Carbonization MOF/CNF Aerogel for High-Performance Microwave Absorption and Thermal Camouflage. *Carbon* **2025**, *243*, 120485.
186. Zhang, F.; Li, N.; Shi, J.-F.; et al. Cation Bimetallic MOF Anchored Carbon Fiber for Highly Efficient Microwave Absorption. *Small* **2024**, *20*, e2312135.
187. Feng, W.; Liu, Y.; Bi, Y.; et al. Recent Advancement of Magnetic MOF Composites in Microwave Absorption. *Synth. Met.* **2023**, *294*, 117307.
188. Fu, C.; Zhou, H.; Tan, L.; et al. Microwave-Activated Mn-Doped Zirconium Metal–Organic Framework Nanocubes for Highly Effective Combination of Microwave Dynamic and Thermal Therapies against Cancer. *ACS Nano* **2018**, *12*, 2201–2210.
189. Wang, D.; Wu, Q.; Tan, L.; et al. Tumor Microenvironment-Responsive Nanoregulator CoMnMOF Superparticles for Enhanced Microwave Dynamic Therapy via Multi-Pronged Amplification of Reactive Oxygen Species. *J. Colloid Interface Sci.* **2025**, *697*, 137963.
190. Yue, K.; Wei, Y.; Jin, X.; et al. Molecular Mechanism of Thermal Sensitization Effect of Potential Materials for Microwave Hyperthermia. *Mol. Simul.* **2020**, *46*, 932–941.
191. Li, S.; Chen, Z.; Tan, L.; et al. MOF@COF Nanocapsule for the Enhanced Microwave Thermal-Dynamic Therapy and Anti-Angiogenesis of Colorectal Cancer. *Biomaterials* **2022**, *283*, 121472.
192. Zhou, H.; Fu, C.; Chen, X.; et al. Mitochondria-Targeted Zirconium Metal-Organic Frameworks for Enhancing the Efficacy of Microwave Thermal Therapy against Tumors. *Biomater. Sci.* **2018**, *6*, 1535–1545.
193. Ndamyabera, C.A.; Langmi, H.W. Recent Developments in Organic Radical Inclusion in MOFs and Radical MOFs. *ChemistryOpen* **2025**, *14*, e202500069.
194. Khalil, I.E.; Fonseca, J.; Reithofer, M.R.; et al. Tackling Orientation of Metal-Organic Frameworks (MOFs): The Quest to Enhance MOF Performance. *Coord. Chem. Rev.* **2023**, *481*, 215043.
195. Bathula, S.; Thottathil, S.; Puttaiahgowda, Y.M. MOFs and MOF-Based Composites for the Adsorptive Removal of Ciprofloxacin. *Macromol. Mater. Eng.* **2025**, *310*, 2400238.
196. Gupta, D.K.; Kumar, S.; Wani, M.Y. MOF Magic: Zirconium-Based Frameworks in Theranostic and Bio-Imaging Applications. *J. Mater. Chem. B* **2024**, *12*, 2691–2710.
197. Chen, Z.; Guo, W.; Liang, T.; et al. Logic Gate Controlled Theranostic Nanoagents for in Situ Microwave Thermal Therapeutic Efficacy Evaluation. *Biomaterials* **2023**, *302*, 122299.

198. Liu, N.; Ren, X.; Guo, W.; et al. Microwave-Responsive, Energy-Metabolism-Regulating Nanosystem for Tumor Treatment through Co-Promotion of Cuproptosis/Ferroptosis. *J. Colloid Interface Sci.* **2026**, *704*, 139424.
199. Zhao, L.; Tan, L.; Wu, Q.; et al. A Two-Stage Exacerbated Hypoxia Nanoengineering Strategy Induced Amplifying Activation of Tirapazamine for Microwave Hyperthermia-Chemotherapy of Breast Cancer. *J. Colloid Interface Sci.* **2024**, *659*, 178–190.
200. Wang, Q.; Zhu, X.; Meng, X.; et al. Lenvatinib Delivery Using a Gd/Fe Bimetallic MOF: Enhancing Antitumor Immunity Following Microwave-Based Thermal Therapy. *Acta Biomater.* **2023**, *172*, 382–394.
201. Ma, S.; Wang, Q.; Zhang, Y.; et al. Targeted Microwave Sensitizers Reprogram Cancer-Associated Fibroblasts via Nitric Oxide Delivery to Potentiate Hepatocellular Carcinoma Therapy. *J. Control. Release* **2026**, *394*, 114900.
202. Zhu, X.; He, C.; Tan, L.; et al. An Fe-Cu Bimetallic Organic Framework as a Microwave Sensitizer for Treating Tumors Using Combined Microwave Thermotherapy and Chemodynamic Therapy. *J. Pharm. Anal.* **2024**, *14*, 100952.
203. Zhao, L.; Zhang, W.; Wu, Q.; et al. Lanthanide Europium MOF Nanocomposite as the Theranostic Nanoplatform for Microwave Thermo-Chemotherapy and Fluorescence Imaging. *J. Nanobiotechnology* **2022**, *20*, 133.
204. Guo, W.; Niu, M.; Chen, Z.; et al. Programmed Upregulation of HSP70 by Metal-Organic Frameworks Nanoamplifier for Enhanced Microwave Thermal-Immunotherapy. *Adv. Healthcare Mater.* **2022**, *11*, 2201441.
205. Zhang, D.; Zhang, Y.; Luo, Y.; et al. Perfluoropentane/Apatinib-Encapsulated Metal–Organic Framework Nanoparticles Enhanced the Microwave Ablation of Hepatocellular Carcinoma. *Nanoscale Adv.* **2023**, *5*, 4892–4900.
206. Xue, T.; Xu, C.; Wang, Y.; et al. Doxorubicin-Loaded Nanoscale Metal-Organic Framework for Tumor-Targeting Combined Chemotherapy and Chemodynamic Therapy. *Biomater. Sci.* **2019**, *7*, 4615–4623.
207. Wang, L.; Yu, X.; Li, X.; et al. MOF-Derived Yolk-Shell Ni@C@ZnO Schottky Contact Structure for Enhanced Microwave Absorption. *Chem. Eng. J.* **2020**, *383*, 123099.
208. Cui, X.; Ruan, Q.; Zhuo, X.; et al. Photothermal Nanomaterials: A Powerful Light-to-Heat Converter. *Chem. Rev.* **2023**, *123*, 6891–6952.
209. Paściak, A.; Marin, R.; Abiven, L.; et al. Quantitative Comparison of the Light-to-Heat Conversion Efficiency in Nanomaterials Suitable for Photothermal Therapy. *ACS Appl. Mater. Interfaces* **2022**, *14*, 33555–33566.
210. Han, C.; Wu, F.; Lin, Q.; et al. Microwave-Induced Energy Activation: Mechanisms and Material Advances. *iScience* **2026**, *29*, 115172.
211. Li, Q.; Liao, H.; Jiang, L.; et al. Low-Dimensional Transition Metal Sulfides Empower Emergent Microwave Attenuation Materials: Nanoarchitectonic, Progress, and Outlook. *Mater. Res. Bull.* **2025**, *184*, 113273.
212. Zhao, L.; Jiang, M.; Xu, Z.; et al. Selective Thermotherapy of Tumor by Self-Regulating Photothermal Conversion System. *J. Colloid Interface Sci.* **2022**, *605*, 752–765.
213. Chen, X.; Gao, H.; Tang, Z.; et al. Optimization Strategies of Composite Phase Change Materials for Thermal Energy Storage, Transfer, Conversion and Utilization. *Energy Environ. Sci.* **2020**, *13*, 4498–4535.
214. Su, Z.; Kong, L.; Dai, Y.; et al. Bioresponsive Nano-Antibacterials for H_2S-Sensitized Hyperthermia and Immunomodulation against Refractory Implant–Related Infections. *Sci. Adv.* **2022**, *8*, eabn1701.
215. Zhou, G.; Wang, Y.S.; Jin, Z.; et al. Porphyrin-Palladium Hydride MOF Nanoparticles for Tumor-Targeting Photoacoustic Imaging-Guided Hydrogenothermal Cancer Therapy. *Nanoscale Horiz.* **2019**, *4*, 1185–1193.
216. Kumar, D.; Singh, H.; Deep, A.; et al. Microneedles-Integrated Photothermal-Based Combinational Therapeutics for Cancer Treatment. *Adv. Mater. Technol.* **2026**, *11*, e71039.
217. Xia, Z.; Hu, Y.; Zhang, W.; et al. Overcoming Biological Barriers with a Microwave-Sensitizing Nanomotor for Empowering Microwave Thermal Immunotherapy. *ACS Appl. Mater. Interfaces* **2026**, *18*, 11022–11036.
218. Zhang, J.; Wang, K.; Xu, S.; et al. Silk Fibroin-Coated Nano-MOFs Enhance the Thermal Stability and Immunogenicity of HBsAg. *ACS Appl. Mater. Interfaces* **2024**, *16*, 8346–8364.
219. Hu, X.; Li, R.; Liu, J.; et al. Engineering Dual-Responsive Prodrug-MOFs as Immunogenic Cell Death Initiator for Enhancing Cancer Immunotherapy. *Adv. Healthcare Mater.* **2024**, *13*, e2302333.